9950-377

CONCEPTUAL DESIGN STUDY OF CONCENTRATOR ENHANCED SOLAR ARRAYS FOR SPACE APPLICATIONS

Final Report of First Contract Extension Phase
20 March 1980

2 kW Si and GaAs Systems at 1 AU

(NASA-CR-163046) CONCEPTUAL DESIGN STUDY OF CONCENTRATOR ENHANCED SOLAR ARRAYS FOR SPACE APPLICATIONS. 2kW Si AND GaAs SYSTEMS AT 1 AU Final Report (Hughes Aircraft Co.) 55 p HC A04/MF A01 CSCL 19A G3/44

N80-28863

Unclas 28288

JPL CONTRACT NO. 955194
HUGHES REF NO. E3256

HUGHES
HUGHES AIRCRAFT COMPANY

9950-377

HUGHES AIRCRAFT COMPANY

Technology Division

Space and Communications Group

El Segundo, California

CONCEPTUAL DESIGN STUDY OF CONCENTRATOR ENHANCED SOLAR ARRAYS FOR SPACE APPLICATIONS

FINAL REPORT - FIRST CONTRACT EXTENSION PHASE
20 MARCH 1980

(2 kW Si and GaAs Systems at 1 AU)

JPL Contract No. 955194
HAC Ref. No. E3256

Approved: I. Baker
I. Baker
Program Manager
20 March 1980

This work was performed for the Jet Propulsion Laboratory, California Institute of Technology, sponsored by the National Aeronautics and Space Administration under Contract NAS-7-100

FINAL REPORT, FIRST CONTRACT EXTENSION

(2kW Si and GaAs Systems at 1 AU)

CONTENTS

1.0 INTRODUCTION

2.0 SUMMARY AND CONCLUSIONS

3.0 OPTICAL ANALYSIS

4.0 THERMAL ANALYSIS

5.0 SOLAR CELL ANALYSIS

6.0 SYSTEM EVALUATION

7.0 WEIGHT ANALYSIS

1.0 INTRODUCTION

This document is the final report of the first extension to JPL Contract No. 955195, "Conceptual Design Study of Concentrator Enhanced Solar Arrays for Space Applications." Technical effort on the original contract, prior to the add-on effort herein described, was covered in a two volume document which was designated an "Interim Final Report" and dated 15 May 1979. The detailed statement of work for the add-on task is described in JPL Contract, Unilateral Modification Number 1.

The original contract effort studied several very large 25 kW silicon cell systems for use from 1 to 6 AU and one 2 kW system in the same solar distance range. On the other hand, the contract extension effort described in this report was restricted to the study of 2 kW systems at 1 AU only. More specifically, the contract extension effort called for an investigation of the following:

1. Concentrator enhancement of a deployable, thin, gallium arsenide cell array in geosynchronous orbit for 10 years, in conjunction with a two dimensional flat plat trough (2D-FPT) concentrator sometimes referred to as a V trough, (Figure 1.0-1) and also with a multiple flat plate concentrator (MFPC) as proposed in the original contract effort (Figure 1.0-2). Each concentrated system considered is sized to generate 2kW at EOL. The GaAs cells are 16% efficient at BOL and 50 microns thick with a 75 micron fused silica cover.

2. Concentrator enhancement of a conventional silicon solar cell array on a rigid substrate in geosynchronous orbit for 10 years, considering a 2D-FPT concentrator only. The substrate is similar to that used on the FLTSATCOM while the cells are 13% efficient, BOL, 200 microns thick with 150 micron fused silica cover. Again, the system is required to generate 2kW at EOL for every concentration level considered.

In this parametric study, the total output power was held constant (at 2kW) so that the effect of various levels of concentration was to change the array area required. This differed from the approach used in the original contract effort, where the unconcentrated array area was held constant allowing the power output to change with concentration ratio.

As in the original contract effort, the extension effort considered the effect of a spectrally selective "cold mirror" coating on the performance of the concentrated system. However, since the completion of the original contract effort, data on an improved performance cold mirror coating became available (see Section 3.0, Optical Analysis). The improved coating was included as a parameter in this study along with vapor deposited aluminum (VDA) which produces an ordinary uniformly reflective mirror.

Of primary interest in this contract extension effort is the determination of the degree to which the power to mass ratio of a concentrated array may be superior, if at all, to an unconcentrated array of equal power. Thus, for the systems studied, the most significant "yardstick" for judging one concentrated system concept to be superior to or more desirable than another is an improvement in specific power (power to mass). Of secondary importance to specific power, however, is the reduction in the initial array area required for a given power output. On the assumption that the solar cells themselves may be among the most costly elements of a photovoltaic power system, significant reductions in array area needed to achieve a required power may be of interest even with little or no accompanying improvement in specific power.

For this reason, the effect of concentrators on required array area was also studied and reported.

2.0 SUMMARY AND CONCLUSION

2.1 Thin, Deployable, Gallium Arsenide Arrays

Figures 2.0-1 and 2.0-2 show the effect of concentration level on specific power for both concepts investigated. As expected,, both concepts exhibit an optimum C_g for maximum power to mass performance. Referring to Figure 2.0-1 for the 2D-FPT, at EOL, a maximum specific power of 143 watts/kg is obtained at C_g = 2.5. With no concentration, approximately 120 watts/kg are delivered at EOL. Therefore, the 2D-FPT produces an improvement in specific power of the unconcentrated array of about 19%.

By constrast, Figure 2.0-2 shows that for the MFPC, the maximum specific power (achieved at C_g = 2.0 for the passive design or C_g = 3.0 for the semi-active version) is only about 50 watts/kg. This is less than half of what is delivered by the unconcentrated but front-lit array. The reason for the poor performance is that the MFPC is a back-lit design. Mirrors and attendant mass are required to provide any sunlight on the array at all, even at C_g = 1.

For both GaAs systems studied, reduction in array area to achieve a 2kW system output after a 10 year life is dramatic. Figures 6.0-1 and 6.0-2 illustrate this result. As expected, both concepts exhibit an optimum concentration ratio for maximum area reduction. Concentration beyond the optimum produces diminishing returns as the effect of a decrease in efficiency due to temperature effects dominates the effect of increased illumination from the increasing concentration. With the 2D-FPT concept, Figure 6.0-1, the results are the same for both coatings considered. The optimum concentration ratio is approximately C_g = 5 and produces a reduction in area of 55%. The curves include the effect of the 10 year radiation exposure on the areas required. This effect was found to be between 31% and 36% array area increase to compensate for radiation degradation; the specific amount depending upon the concentration level and coating.

For the MFPC concept, Figure 6.0-2, VDA coated mirrors produced a maximum area reduction at $C_g = 5$ of about 58%. This result is almost identical to that produced by the much more mechanically simple 2D-FPT concept. However, when the improved cold mirror is employed, a reduction in area of 77% is achieved at $C_g = 10$. The improvement from the cold mirror was not obtained with the 2D-FPT apparently because of the nullifying effect of multiple reflections.

In conclusion, for application to a thin GaAs array at 1 AU for 10 years, the 2D-FPT produces a 19% benefit in specific power and a dramatic 55% reduction in array area, while the MFPC design is not only of no benefit, but it is a considerable detriment. The benefit it achieves by reducing array area is duplicated by the simpler 2D-FPT design.

2.2 Conventional Silicon Array on Rigid Substrate

Results for the conventional silicon cell array on a rigid substrate are shown in Figures 6.0-1, 6.0-2, 2.0-1, and 2.0-2. However, for the optimum concentration condition, the pertinent results are summarized in Table 2.0-1.

From the table it can be seen that the improvement in performance due to the concentrator with ordinary mirror coating (VDA) is quite small; 9% increase in specific power, and 13% reduction in array area. When the concentrator mirrors are coated with an improved "cold mirror" coating, the improvements are somewhat more significant; 31% specific power improvement, 27% area reduction. In both cases, a 10 year exposure reduces BOL output by 23%.

FIG. 2.0-1. SPECIFIC POWER OF 2 KW (EOL) 2D-FPT IN GEOSYNCHRONOUS ORBIT

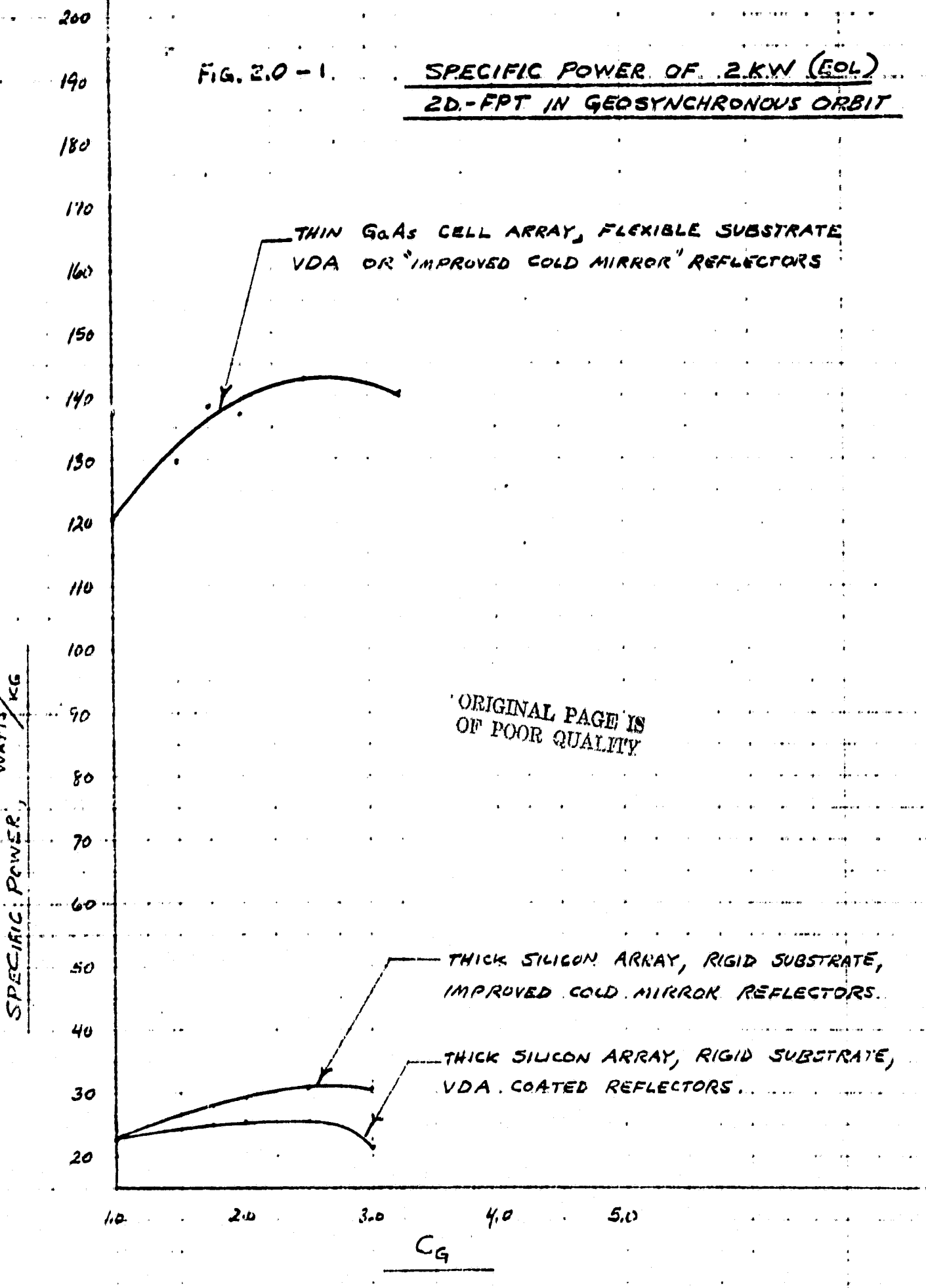

FIG. 2.0-2 2KW (EOL) MFPC IN GEOSYNCHRONOUS ORBIT

THIN GaAs ARRAY

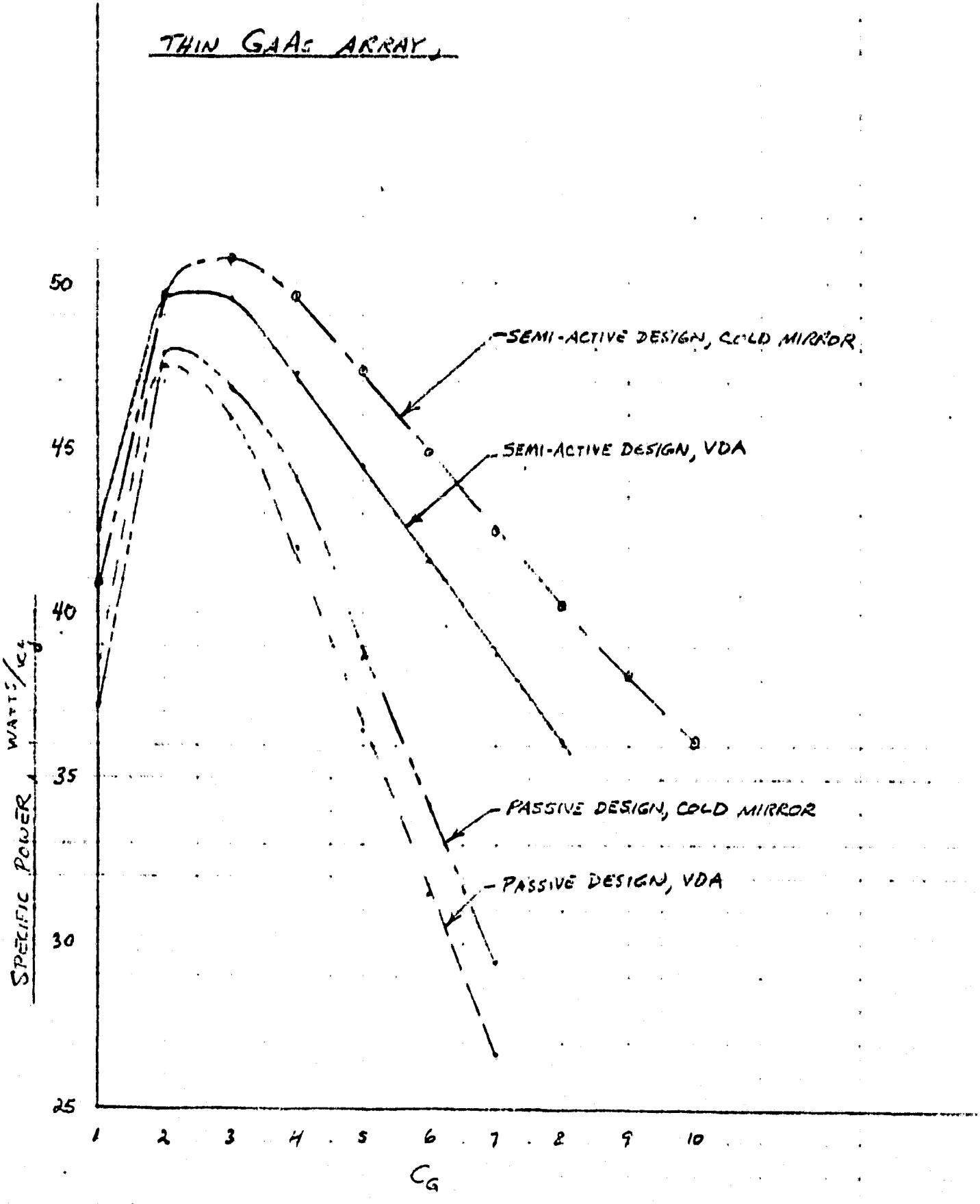

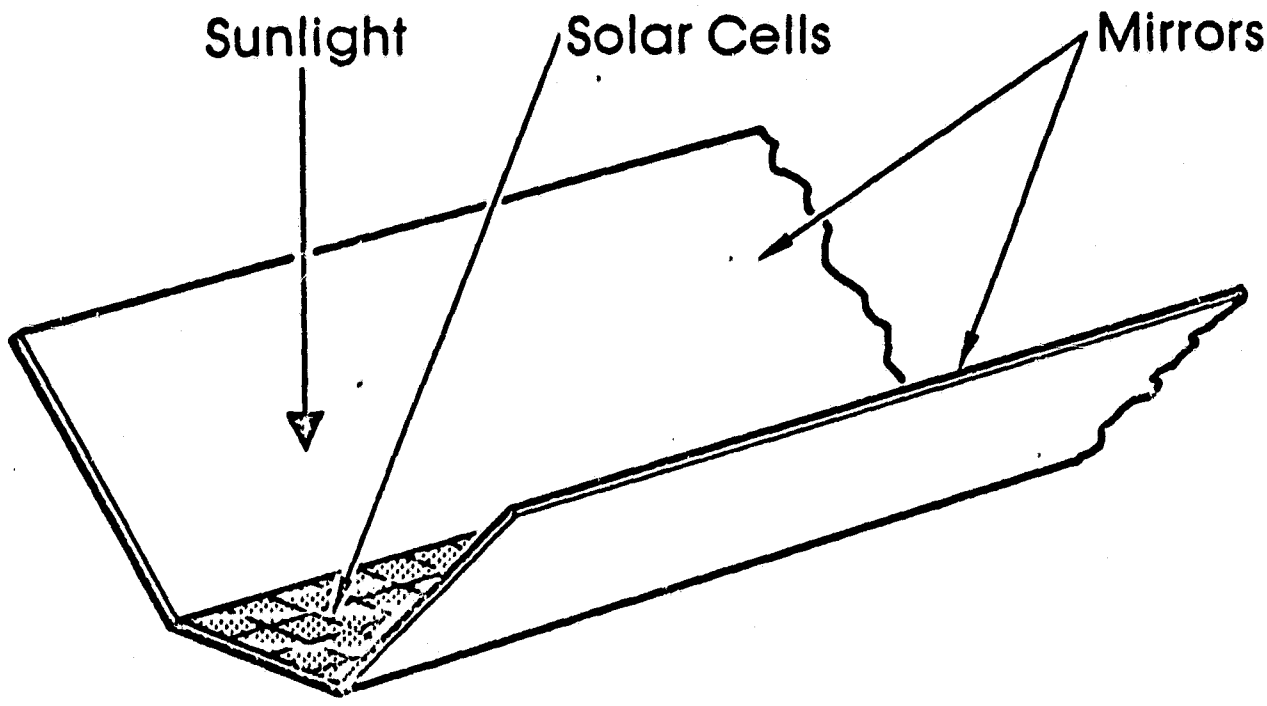

Fig 1.0-1 - Two dimensional front-lit flat plate trough concentrator (2D-FPT)

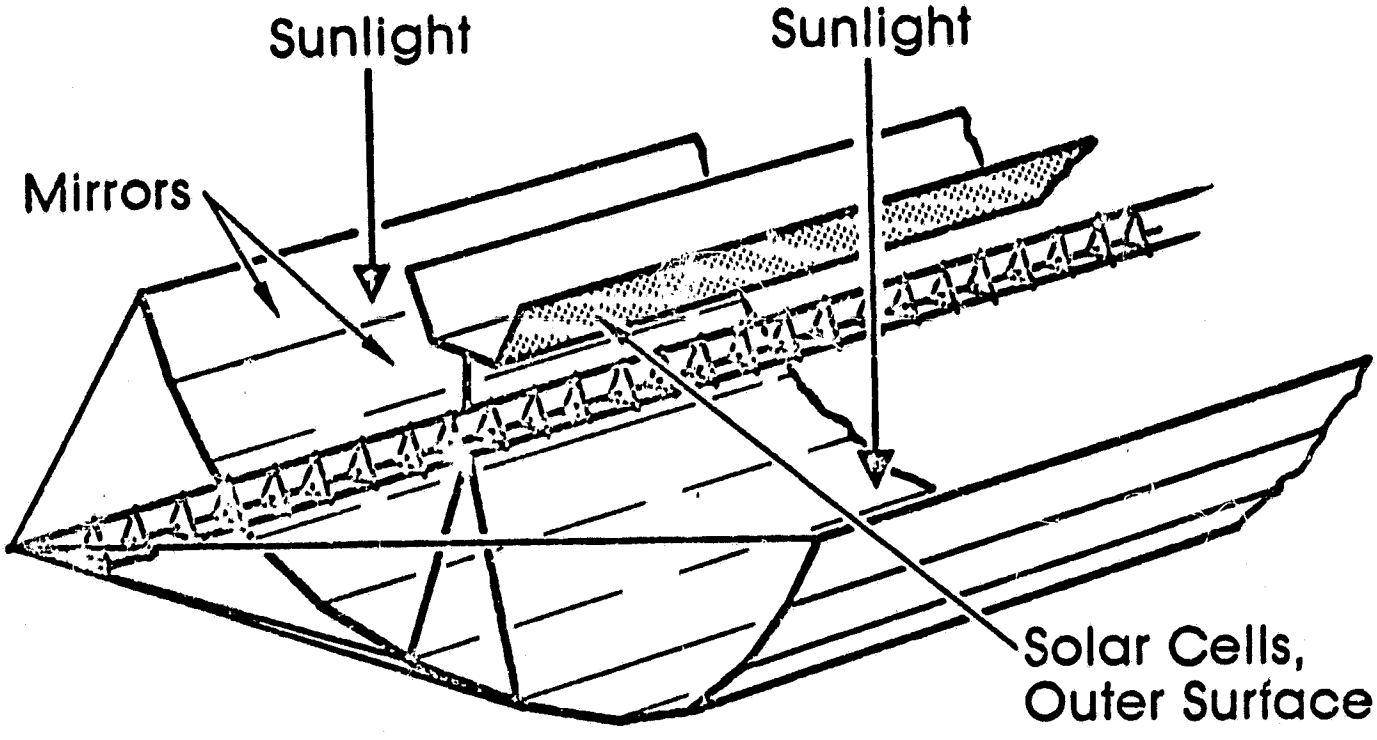

Fig. 1.0-2 - Two-dimensional back-lit multiple flat plate concentrator (MFPC)

TABLE 2.0-1 PERFORMANCE OF 2D-FPT CONCENTRATOR ON CONVENTIONAL Si ARRAY ON RIGID SUBSTRATE

	BEFORE CONCENTRATION					WITH CONCENTRATION TO 2 kW EOL					
	Req'd Array Area Ft^2	Array Wt. Lb.	BOL Power kW	EOL Power kW	EOL Power to Mass Watts/kg	Optimum C_g	Total Wt. Lbs.	BOL Power (kW)	EOL Power to Mass Watts/kg	% Improvement In Power to Mass %	% Improvement In Array Area* %
VDA	186	164 (74.4 kg)	2.24	1.73	23.2 (30.1 BOL)	2.5	174 (78.9kg)	2.41	25.3 (30.5 BOL)	9	13
COLD MIRROR	156	137 (62.1 kg)	1.38	1.45	23.3 (30.3 BOL)	3.0	144 (65.3kg)	2.45	30.6 (37.5 BOL)	31	27

* Based on fact that 214 ft^2 of array area would be required to provide 2 kW EOL power with no concentration.

3.0 Optical Analyses

Optical analyses in the first contract extension phase of the program was restricted to the 2D-FPT; the MFPC having been analyzed in Phase I of the program. Analyses of the flat plate trough was carried out by a series of ray trace studies using the method of images.

The objectives of the analyes were:

1. To determine the maximum concentration ratio possible at each mirror tilt angle while accepting a solar axis misalignment of up to $\pm 5^{o}$ and while maintaining illumination uniformity within specified limits.
   a. When restricted to single reflection
   b. With multiple reflections
   c. With and without oversizing as a means of accommodating sun misalignment.
2. To determine the mirror height required as a function of tilt angle for each of the above design options.
3. To determine the total integrated reflection efficiency for each of two possible mirror coatings. A vapor deposited aluminum (VDA) or an improved OCLI cold mirror.
4. To determine for each design option the percentage of the total received light which is lost, directly received, reflected once, reflected twice, etc. as a function of concentration ratio.
5. To quantify the illumination nonuniformity, if any, for each design option as a function of solar axis misalignment and concentration ratio or tilt angle.

All of the above objectives were accomplished by ray tracing studies using the method of images which will now be described using the sketch in figure 3.0-1. The trough shown in solid line in this figure is a 2D-FPT concentrator while those shown in phantom are mirror images of that concentrator placed side by side. Thus, the array being concentrated together with its images forms a polygon; while the concentrator mirrors and its images are the extensions of radii of this polygon. As an example of the procedure, entering light ray no. 1 strikes the actual concentrator mirror at point a with an angle of incidence $\emptyset$ and is reflected with angle of reflection $\emptyset$ to the opposite mirror striking it at b'. This reflected ray ab' is similarly reflected again to the first mirror striking it at c' and then reflected a third and final time to the array striking it at point d'.

By the method of images, the same information is obtained by simply extending entering light ray no. 1 as a single straight line abcd. As the ray crosses a mirror or mirror image, it leaves the mirror at the same angle to the normal with which it arrived. Therefore, ab = ab', bc = b'c' and cd = c'd'. Any ray so extended which does not strike the array polygon will never reach its target but will eventually be reflected out of the aperture and will be lost. For example, entering light ray no. 2 will never reach the array.

Using such an analysis procedure it was determined that 4 basic design options are available for study, each resulting in a higher concentration ratio and requiring larger mirrors than the next. Figure 3.0-2 describes, as an example, the options for a particular reflector tilt angle and presents data on C_g versus sun pointing error θ for each. The option resulting in the lowest concentration is labeled no. (4). It also requires the shortest mirrors.

14

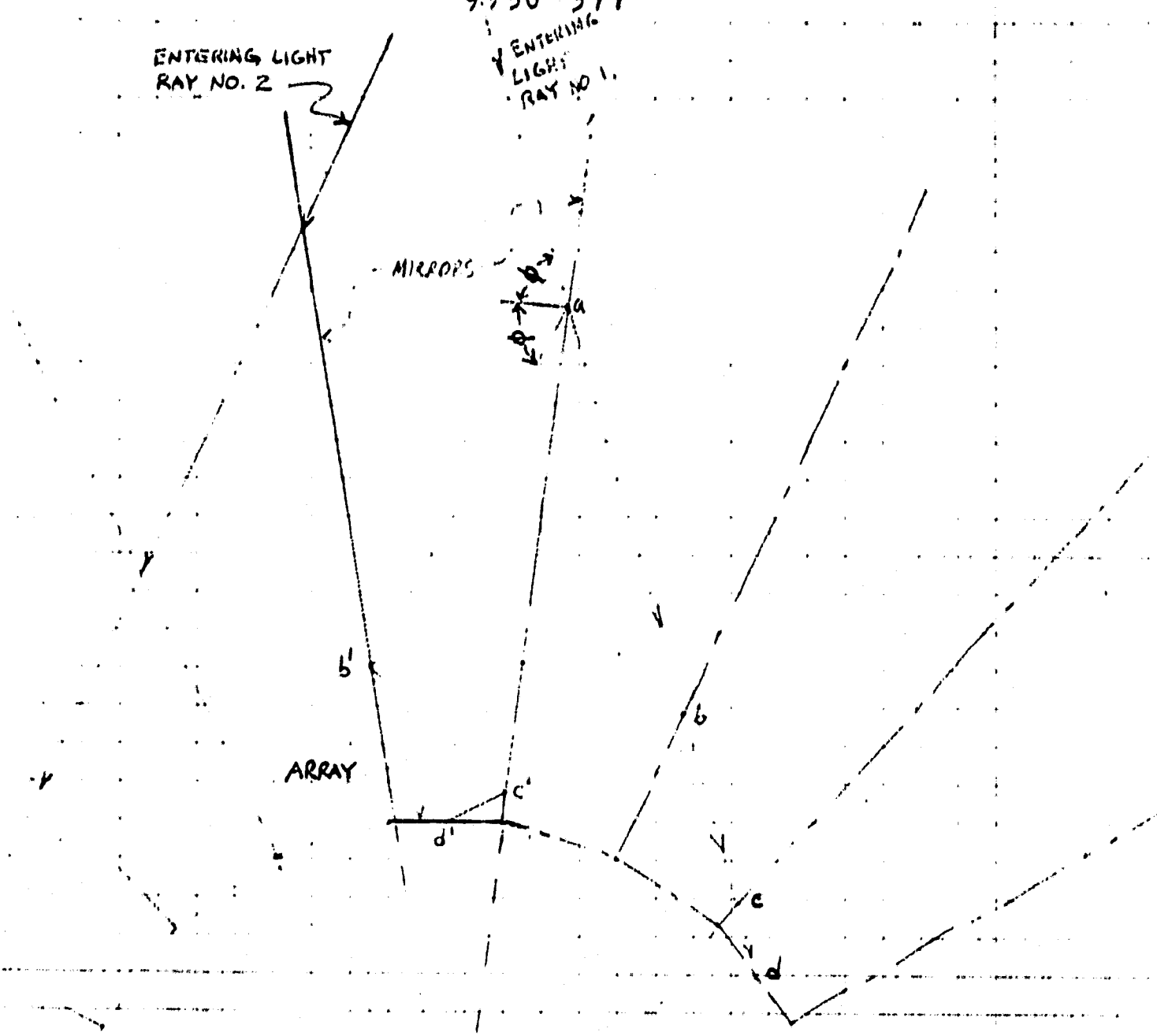

FIGURE 3.0-1 ILLUSTRATION OF THE METHOD OF IMAGES - USED IN RAY TRACING STUDY

FIGURE 3.0-2

DESIGN OPTIONS AVAILABLE FOR A 2D-FPT CONCENTRATOR AT $\phi = 75°$

(TYPICAL FOR OTHER VALUES OF ϕ)

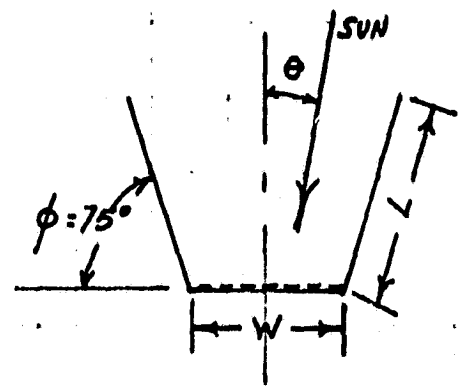

① LOST LIGHT DESIGN FOR $\theta = \pm 5°$
Shows max. C_g possible within $\theta = \pm 5°$ allowing lost light at all θ and multiple reflections.

② DESIGN FOR NO LIGHT LOSS AT $\theta = 0$ ONLY
Shows max. C_g delivered at any θ to $\pm 5°$ when sized for no light loss at $\theta = 0°$ with multiple reflections. light loss does occur for all θ other than $\theta = 0°$.

③ NO LIGHT LOSS DESIGN FOR $\theta = \pm 5°$, MULTIPLE REFLECTIONS
Shows max. C_g possible within $\theta = \pm 5°$. No light loss at any θ and multiple reflections.

④ NO LIGHT LOSS DESIGN FOR $\theta = \pm 5°$, SINGLE REFLECTION
Same as ③ but limited to one reflection.

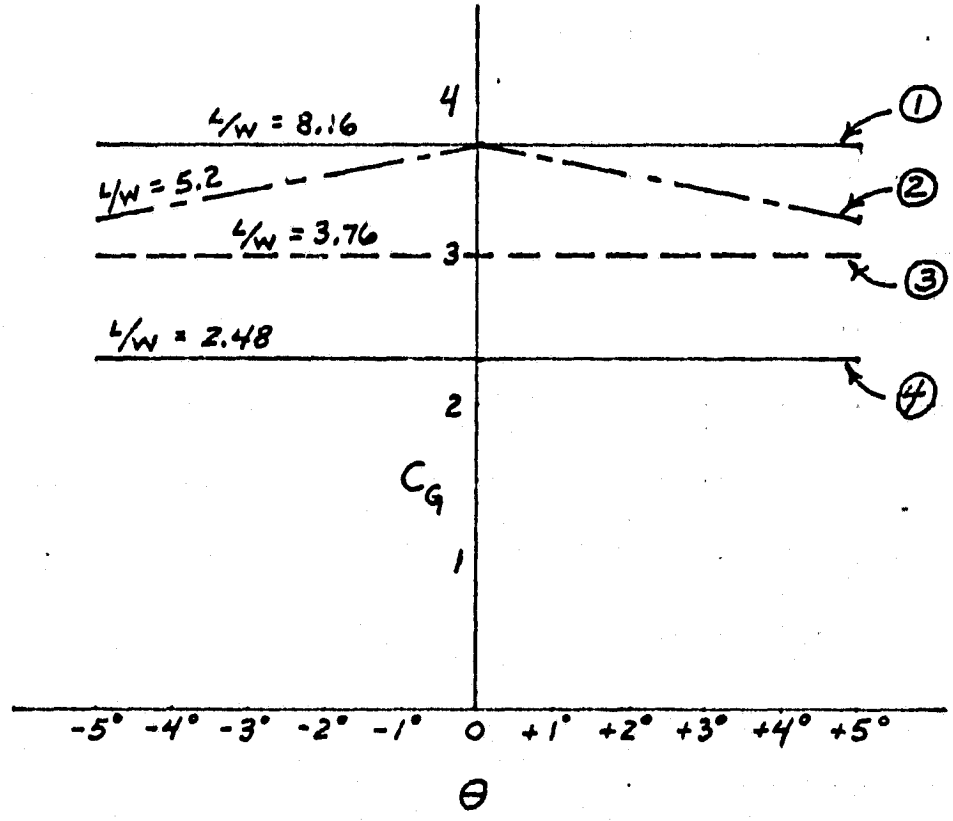

In option ④, the mirror height is selected such that all light entering the aperture even to the $\pm 5^{o}$ extremes of sun misalignment, arrive at the array, no light is lost, and reflected light is only reflected once for minimum reflection losses. Option ③ is the same as option ④, however, multiple reflections are permitted, the number required being dependent upon the mirror tilt angle $\emptyset$. Option ③ gives higher C_g but also has higher reflection losses and longer mirrors than in ④. Option ② is the same as option ③ but it is initially designed for incoming light which is not misaligned. This gives a still larger value of C_g and mirror height. When option ② receives misaligned light, some of the light is lost and the concentration ratio decreases as shown in the figure. Option ① produces the maximum concentration ratio achievable at all values of sun misalignment θ. It accommodates sun axis misalignment by oversizing the mirror height. In this design a constant portion of the entering light is lost for all values of θ including perfect alignment, $\theta = 0^{o}$.

Option ④ was eliminated when it was determined that, for the other options, within the limits of practical mirror heights, the percent of the incoming light which ends up with multiple reflections is relatively small and hence the additional reflection losses are small in these other options while they yield significantly higher C_g than in option ④.

Option ② was eliminated because, as shown in figure 3.0-2, it produces a C_g drop-off as the sun misalignment is increased to $\pm 5^{o}$.

For the remaining options; ① with light loss and ③ with no light loss, curves of C_g versus tilt angle and R (area ratio = 2 L/W) versus tilt angle were generated. (Figures 3.0-3 and 3.0-4). To evaluate these results the effectiveness

ratio $C_{g/R}$ was plotted, Figure 3.0-5. Based on this curve, the optimum design would appear to be option ③ , the no light loss design. However, before this selection was made, the nonuniformity of the final light arriving at the array was evaluated. The results are shown in figure 3.0-6. Based on this result, the no light loss design, option ③, exceeds the ±15% non-uniformity limit of the contract and was eliminated, leaving option ① , the lost light design, as the chosen configuration.

Reflection Efficiency

To evaluate the reflection losses for the chosen design option, 2 mirror coatings were considered. The first, as in the earlier phases of the contract is vapor deposited aluminum (VDA) which produces a conventional highly reflective mirror. The second is an OCLI "cold mirror" coating, a spectrally selective coating which has improved properties over the cold mirror coating previously evaluated in Phase I of this contract. Data on the improved coating was not available during phase I but was made available to HAC by OCLI in time for the contract extension phase. Figure 3.0-7 is a curve of the spectral reflectance of the coating. Figure 3.0-8 is a curve of the normalized response of a typical solar cell while being directly illuminated by AMO standard NASA sunlight, plotted versus wavelength. The overall or integrated effective reflectance (ER) of the OCLI coating was obtained by a simple numerical integration procedure as follows:

$$ER = \frac{\int_{.35}^{1.2} \text{Refl} * (I_{AMO} * R_{es})\, d\lambda}{\int_{.35}^{1.2} (I_{AMO} * R_{es})\, d\lambda} = \frac{.2898}{.3613} = .8029$$

In this integral,

Refl = Reflectance of cold mirror as a function of wavelength λ. (Figure 3.0-7)

I_{AMO} = Thekakara's Solar Spectrum at AMO in watts/cm^2, a function of λ.

Res = Response of solar cell. The short circuit current output in amps per watt of solar intensity, a function of λ.

$(I_{AMO} \cdot Res)$ = Cell response from direct solar light (Figure 3.0-8).

Earlier data available on the reflectance of the OCLI cold mirror coating yielded a value of ER = 0.64. This was the value used in the calculations of the original contract.

FIG. 30-3 MAXIMUM GEOMETRIC CONCENTRATION RATIO FOR 2D-E.P.T. CONCENTRATOR VS MIRROR TILT ANGLE

$\theta = \pm 5°$ (SUN MISALIGNMENT)

MULTIPLE REFLECTIONS

C_G CONSTANT FOR $-5° \leq \theta \leq +5°$

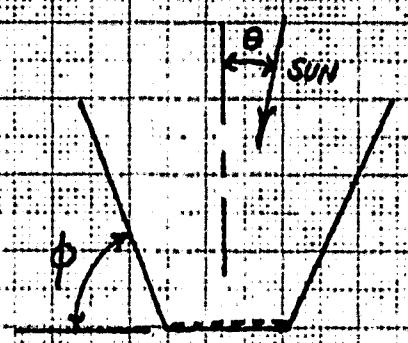

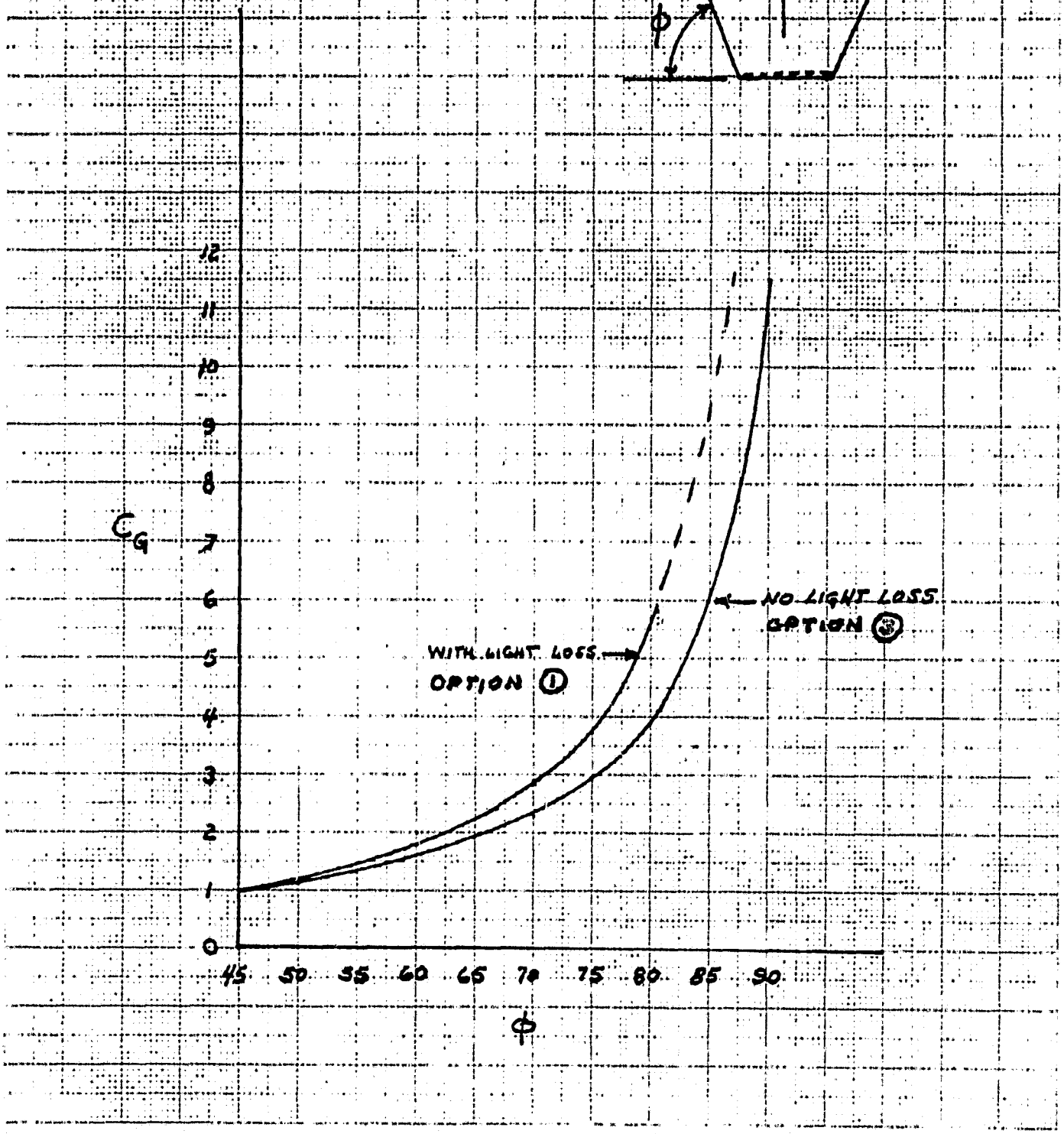

FIG. 3.0-4

AREA RATIO CORRESPONDING TO MAXIMUM C_g CONFIGURATIONS FOR 2D-FPT CONCENTRATOR

$\theta = \pm 5°$

MULTIPLE REFLECTIONS

C_g CONSTANT FOR $-5° \leq \theta \leq +5°$

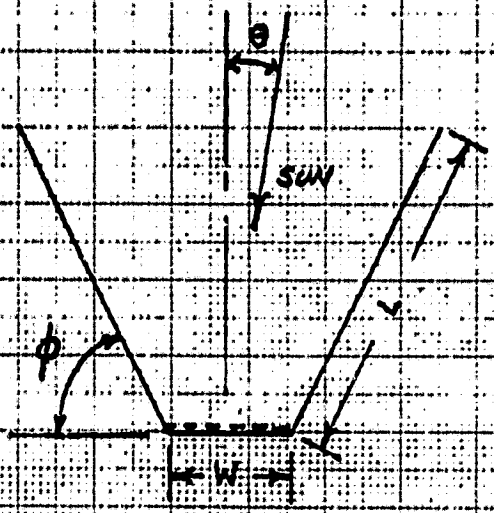

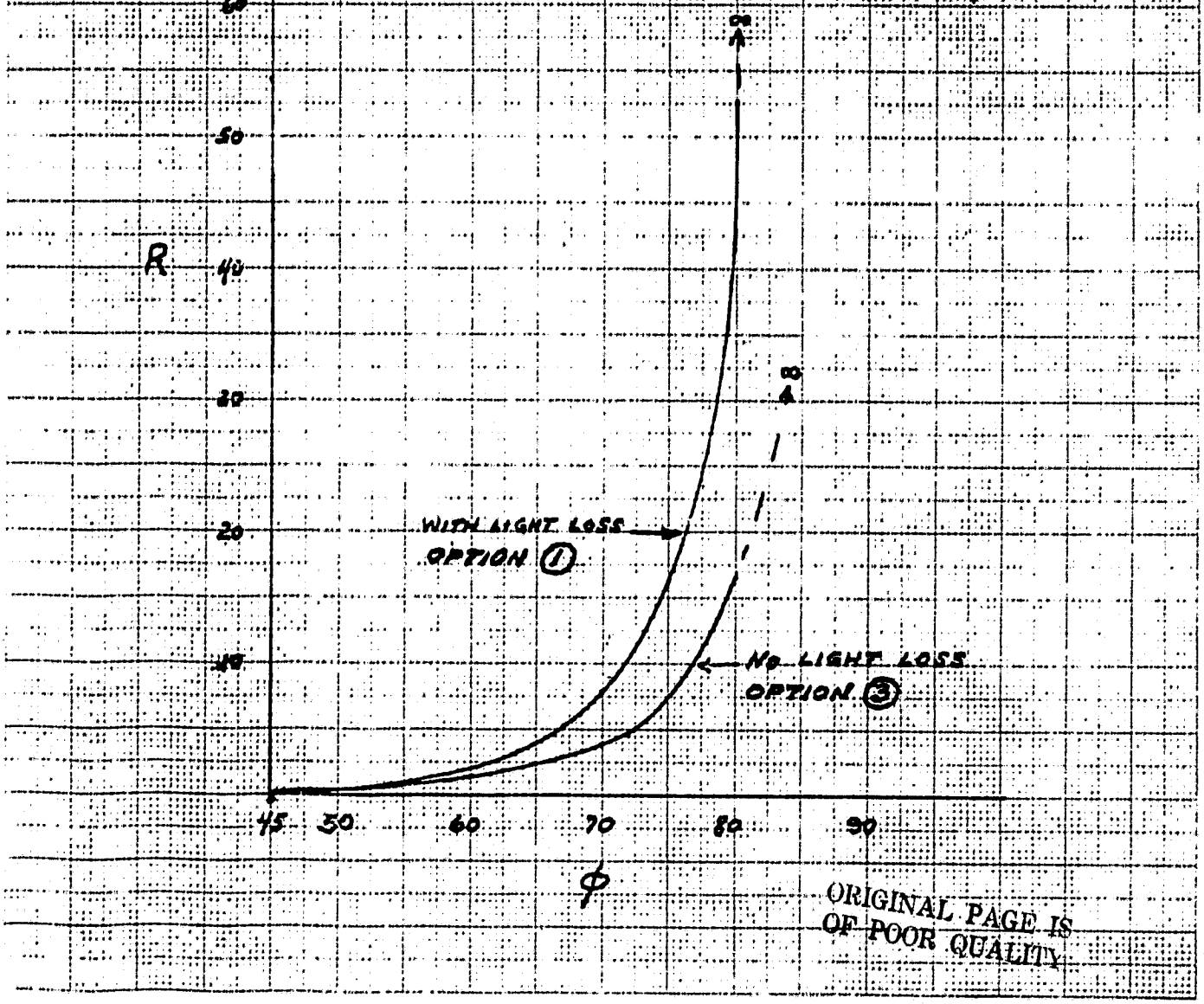

ORIGINAL PAGE IS
OF POOR QUALITY

FIG. 3.0-5 CONCENTRATOR EFFECTIVENESS RATIO, C_G/R, VS. MIRROR TILT ANGLE, ϕ

2D-FPT CONCENTRATOR – MAX. C_G CONFIGURATIONS

$\theta = \pm 6°$, MULTIPLE REFLECTIONS,

C_G CONSTANT FOR $-5° \leq \theta \leq +5°$

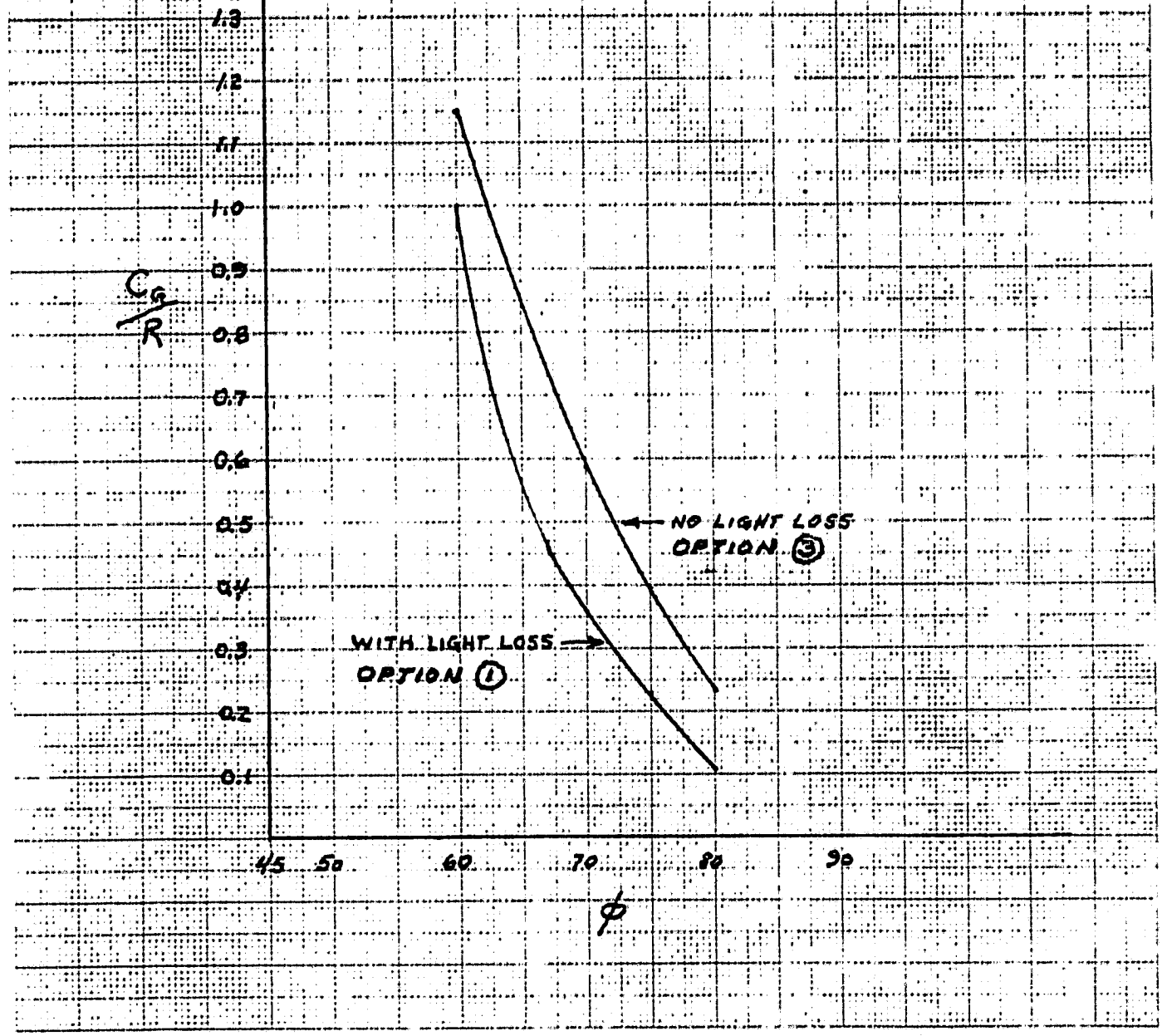

FIG. 3.0-6
ILLUMINATION NONUNIFORMITY VS MIRROR TILT ANGLE ϕ

2D-FPT CONCENTRATOR - MAX C_6 CONFIGURATIONS

$\theta = \pm 5°$
MULTIPLE REFLECTIONS
C_6 CONSTANT FOR $-5° \leq \theta \leq +5°$

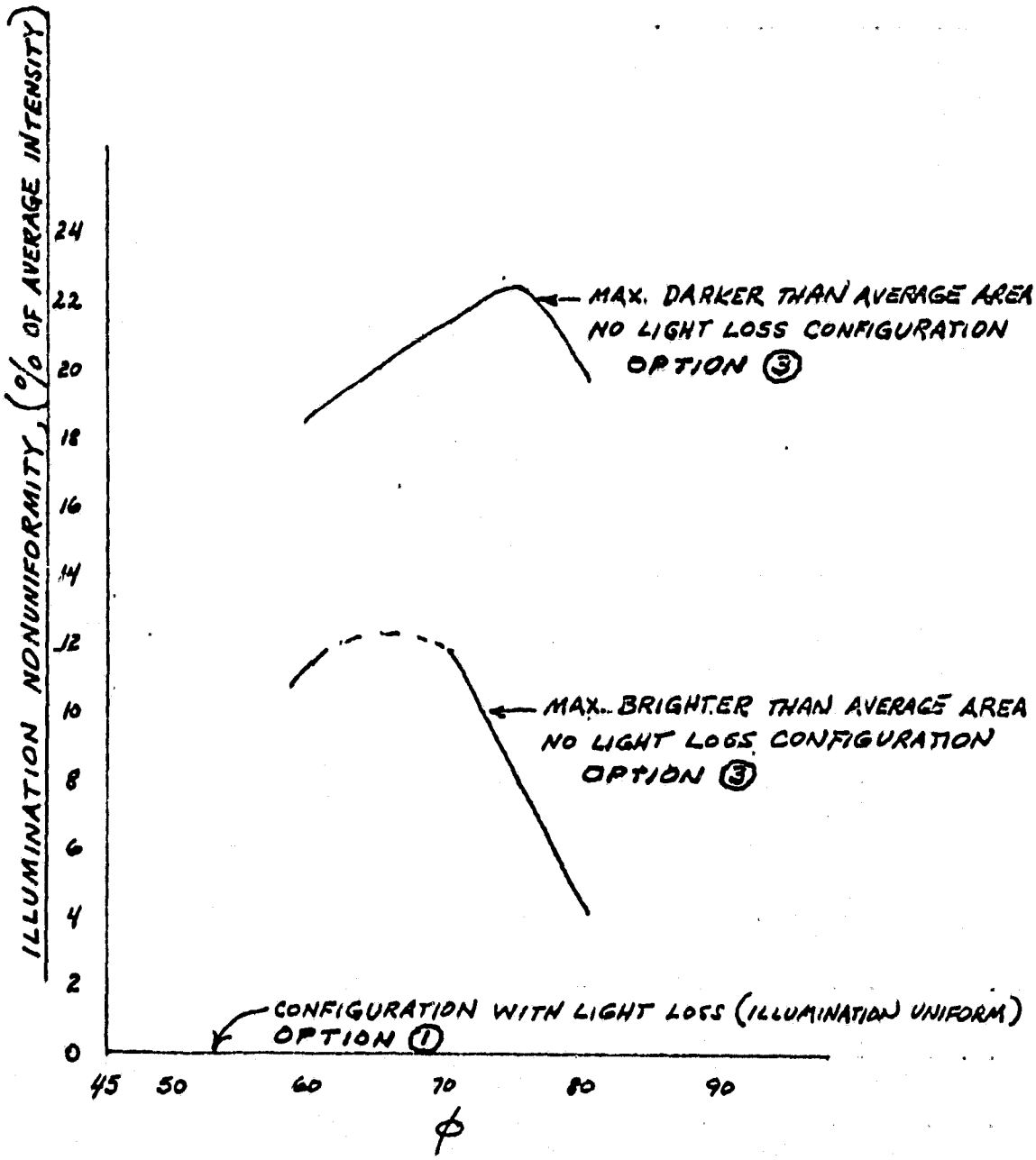

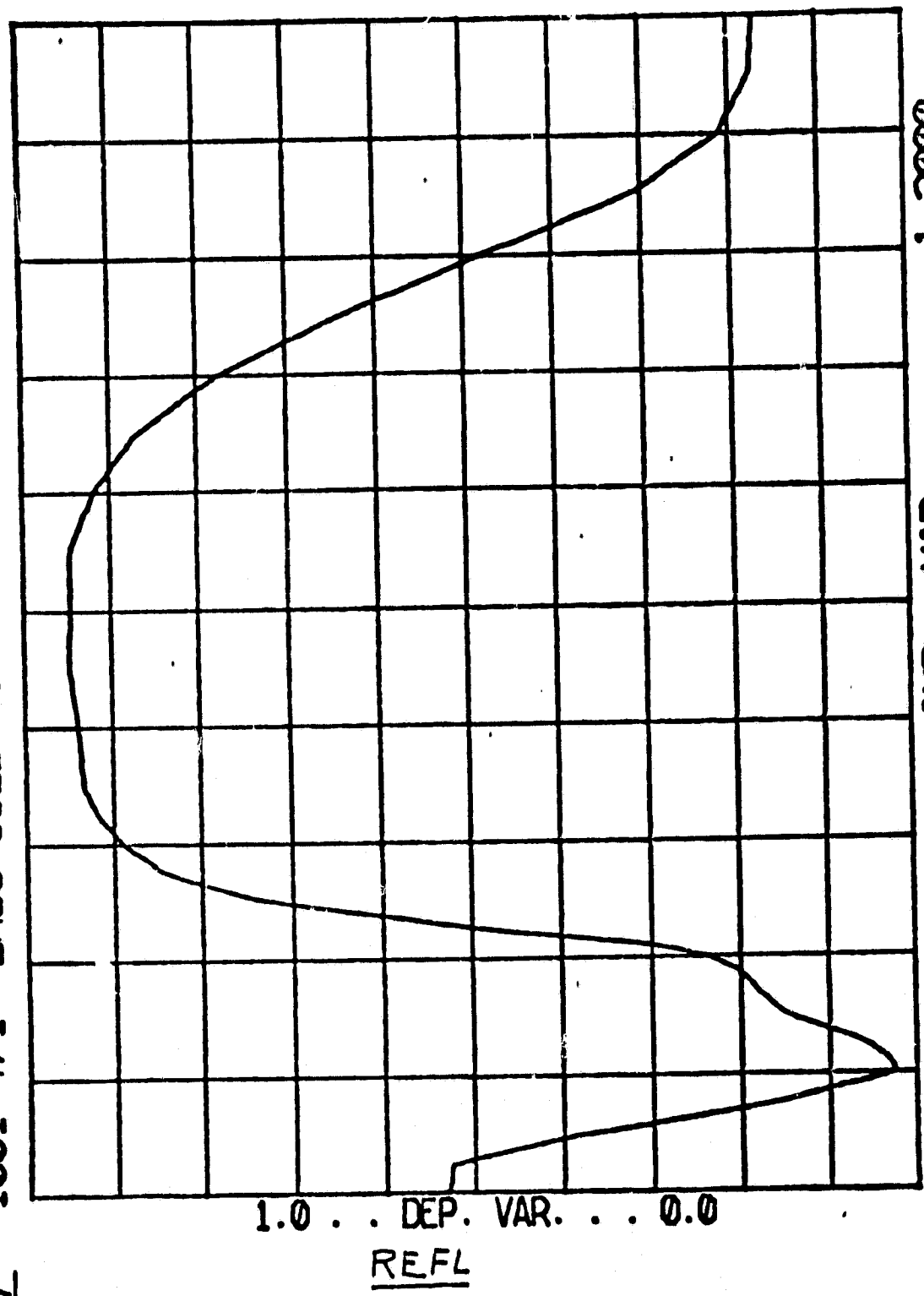

Fig. 3.0-7

Redigitized Data on uniform second color of R_W = $\int R_{eff} * R_{os} * I_{amb}^{D_{65}} / \int R_{os} * I_{amb}^{D_{65}}$ = .802

24

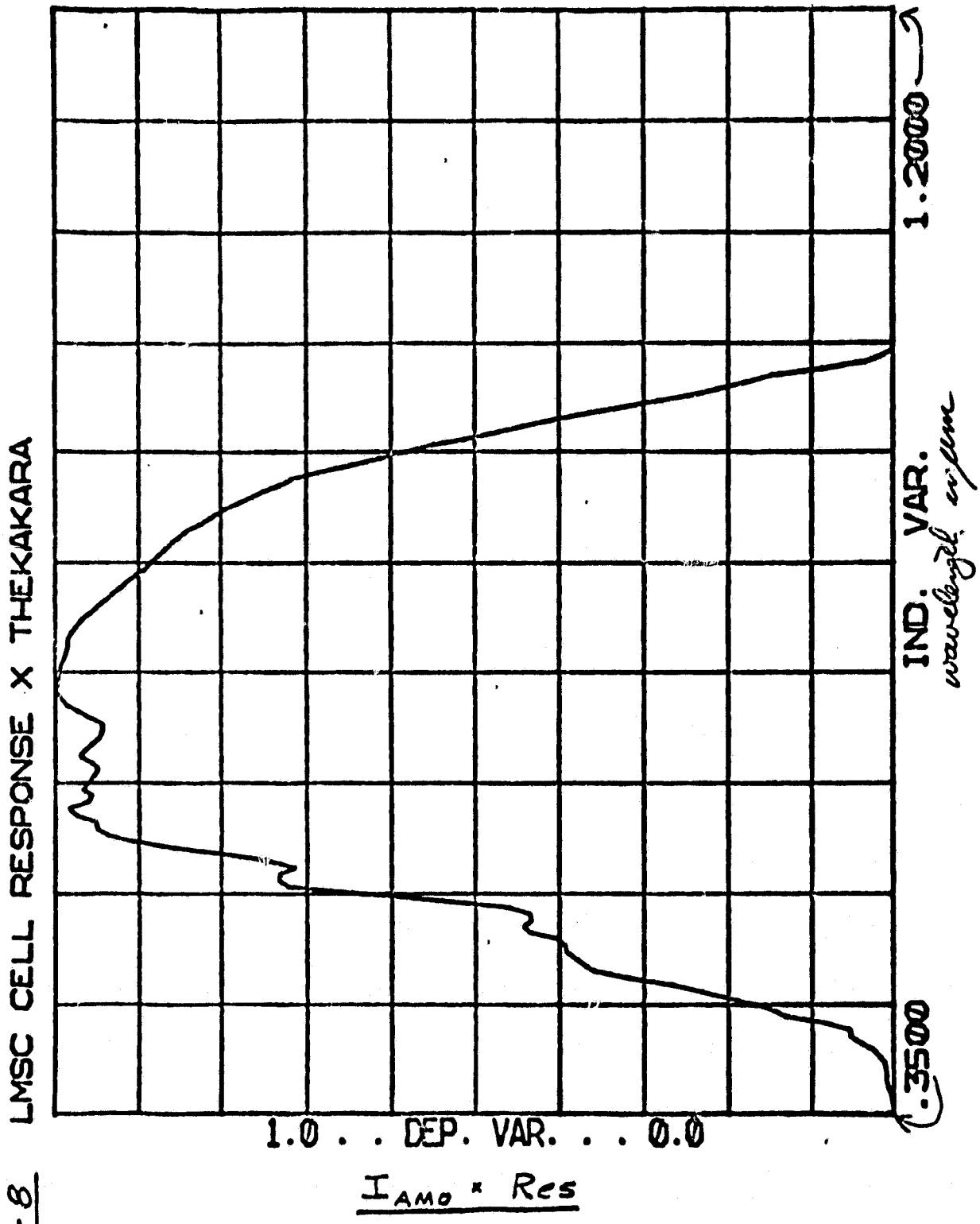
LMSC CELL RESPONSE X THEKAKARA
1.2000
IND. VAR.
wavelength μm
.3500
1.0 . . DEP. VAR. . . 0.0
I_{AMO} x Res

Fig. 3.0-8

For the VDA coating, the effective reflectance was again ER = 0.9 as used and explained in Phase I. Also as in Phase I, an additional loss of 10% due to geometric distortion of the mirrors was included with each reflection.

To determine the final effective concentration ratio for each value of the tilt angle or equivalently for each value of the geometric concentration ratio, it was necessary to determine the apportionment among the number of reflections of the total light entering the aperture. That is, for each value of C_g, a certain percentage of the entering light is directly received by the array, another percentage is reflected once before arriving at the array, a different amount is reflected twice, etc.. This data was readily obtainable using the method of images, and the results for the chosen lost light design, option 1, is shown in figure 3.0-9. For reference, the analogous results for the rejected design option 3 is shown in figure 3.0-10.

Using the data from figure 3.0-9 and accounting for the previously described reflection losses, the total light received at the array was calculated and expressed as a percentage of the total light entering the concentrator aperture; excluding, of course, the lost light. In these calculations, each reflection passes on 81% of the incident light with the VDA (.9 distortion X .9 reflectivity), and 72% with the cold mirror (.9 distortion X .80 reflectivity). The losses go up rapidly with increasing number of reflections. For example, the reflection efficiency for any portion of light reflected three times is $(.72)^3 = 0.37$ for the cold mirror or $(.81)^3 = 0.53$ for the VDA. However, in the selected design, for a practical range of mirror area ratios, the percentage of total light reflected more than once tends to be small. The results of the overall or total reflection efficiency calculations are shown in Figure 3.0-11 for the cold mirror and Figure 3.0-12 for the VDA.

FIG. 3.0-9
APPORTIONMENT OF TOTAL LIGHT RECEIVED BY 2D-FPT CONCENTRATOR, PLOTTED VS C_G

OVERSIZED OR LOST LIGHT CONFIGURATION
$\theta = \pm 5°$ (OPTION ①)

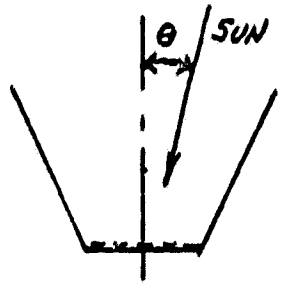

EXAMPLE OF CURVE USE:

ASSUME A LOST LIGHT CONFIGURATION SIZED FOR $C_G = 3$ (VERTICAL DOTTED LINE)
THEN:

% TOTAL LIGHT ENTERING APERTURE	HOW APPORTIONED
24%	LOST
26%	DIRECT TO RECEIVER
40%	RECEIVED AFTER 1 REFLECTION
10%	" " 2 "

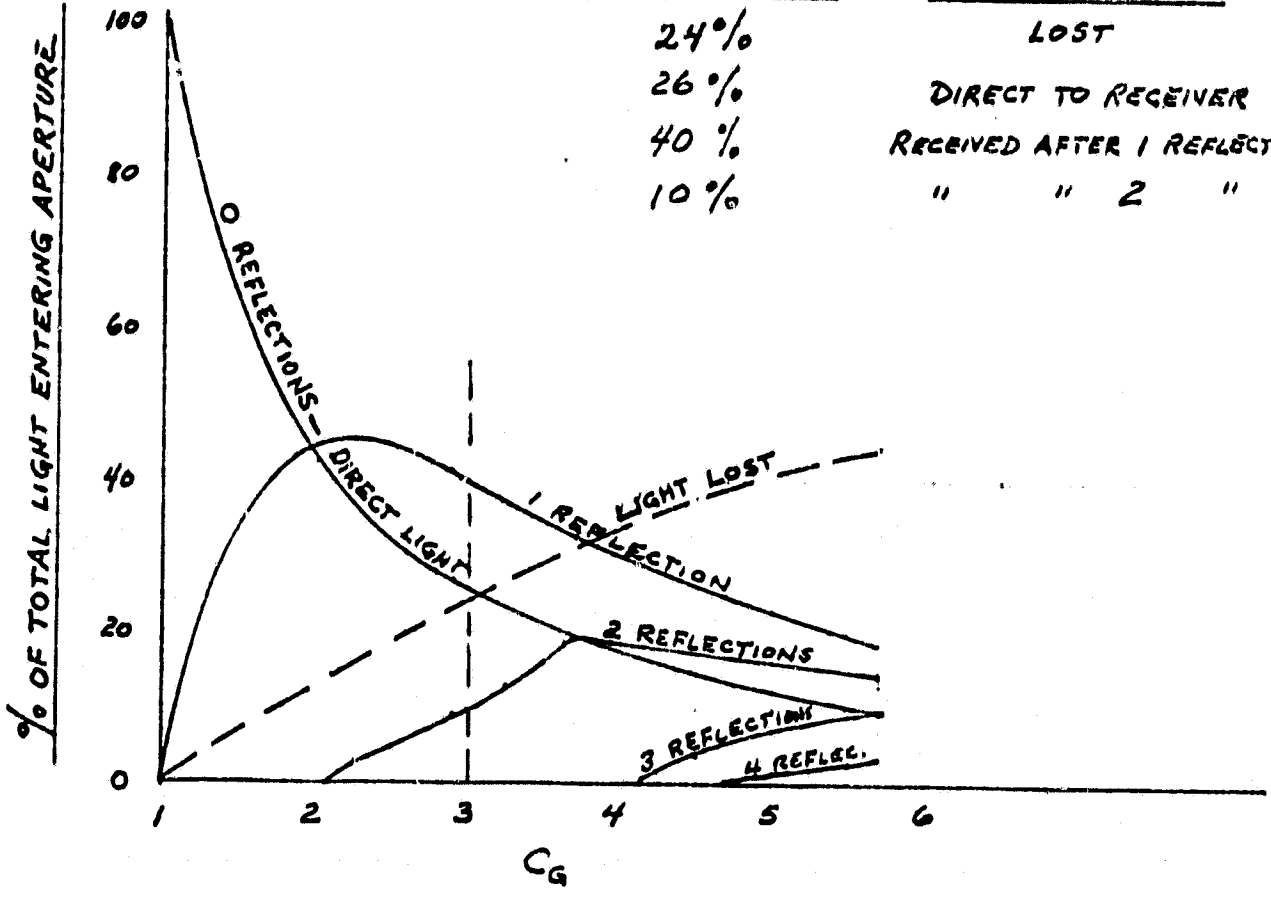

FIG. 3.0-10

PROPORTION OF TOTAL LIGHT RECEIVED BY ARRAY FOR EACH NUMBER OF REFLECTIONS, PLOTTED VS C_G

2D-FPT CONCENTRATOR IN NO LIGHT LOSS CONFIGURATION

$\theta = \pm 5°$ (OPTION ③)

EXAMPLE OF CURVE USE:

ASSUME A ZERO LIGHT LOSS CONFIG. WITH $C_G = 2.5$ (VERTICAL DOTTED LINE)...

THEN:

% TOTAL LIGHT RECEIVED	NO OF REFLECTIONS
40%	0
52%	1
8%	2

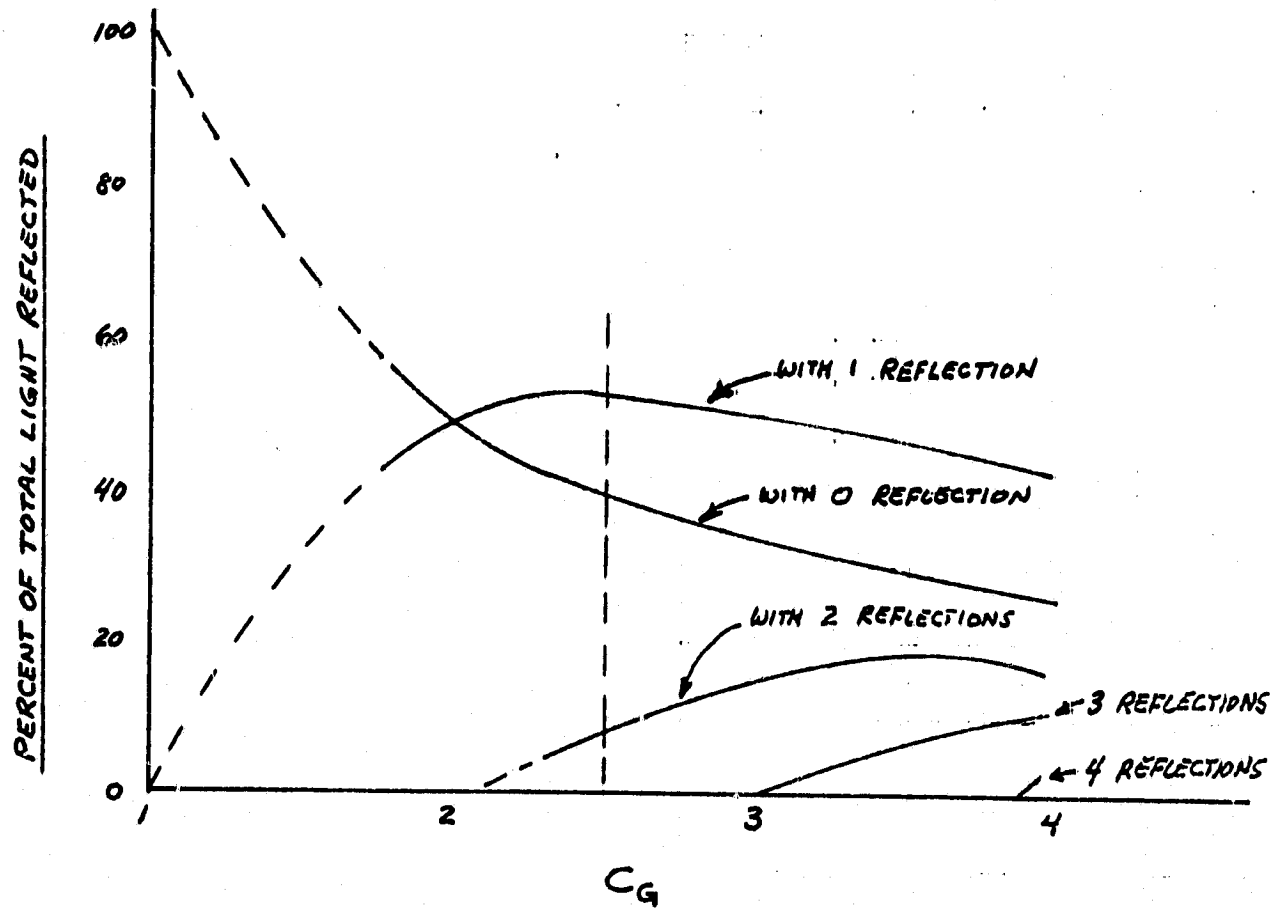

46 1513

28

FIG. 3.0-11

REFLECTION EFFICIENCY FACTOR (RE) FOR 2D-FPT CONCENTRATOR WITH IMPROVED OCLI "COLD MIRROR" REFLECTOR COATING

LOST LIGHT CONFIGURATION, $\theta = \pm 5°$ OPTION (1)
10% LOSS DUE TO MIRROR DISTORTION - EACH REFLECTION
REFLECTIVITY OF COLD MIRROR = 0.80

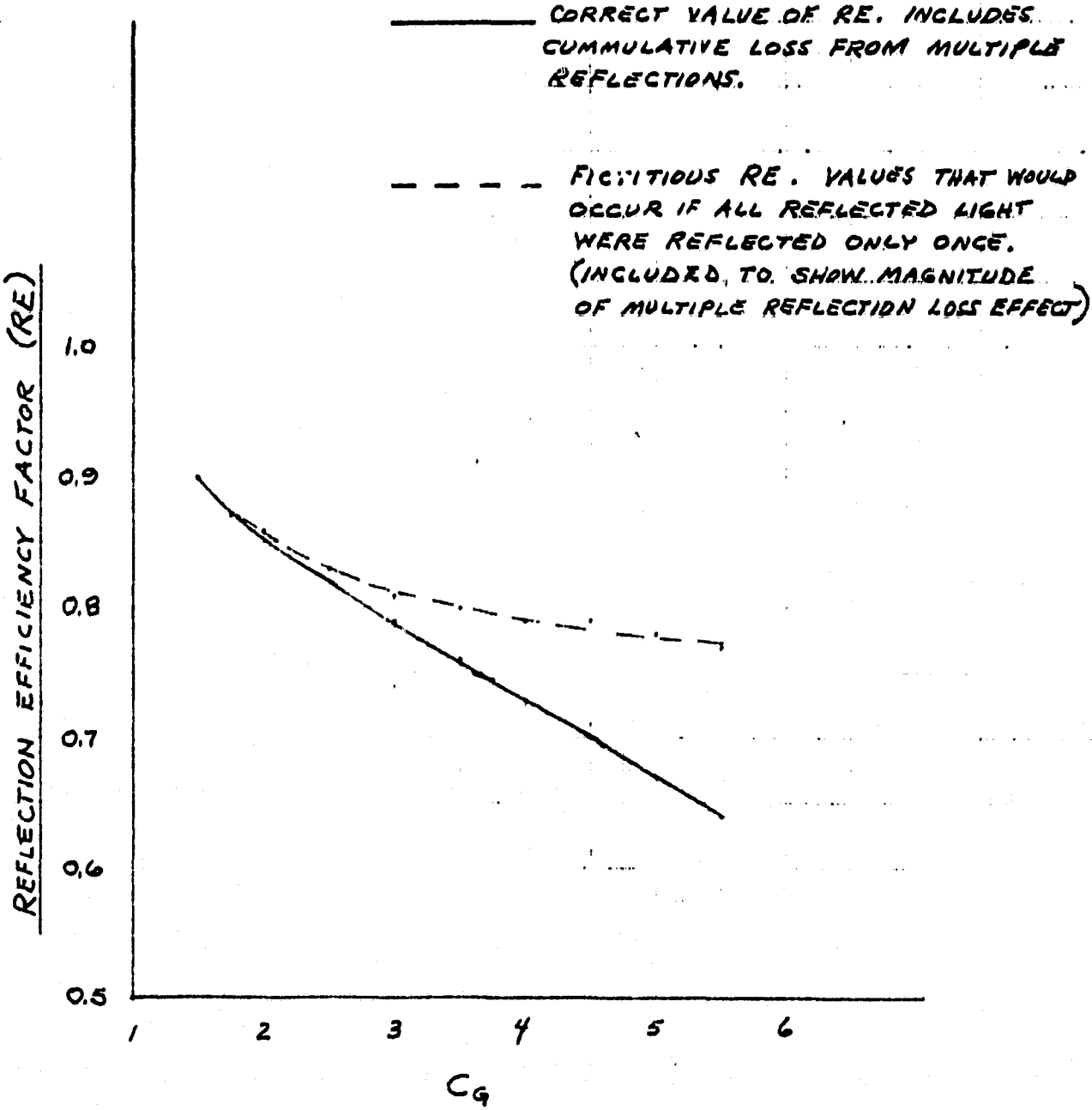

46 1513

24

FIG. 3.0-12

REFLECTION EFFICIENCY FACTOR (RE) FOR 2D-FPT CONCENTRATOR WITH VDA COATED MIRRORS

LOST LIGHT CONFIGURATION, $\theta = \pm 5°$ OPTION ①

10% LOSS, DUE TO MIRROR DISTORTION, WITH EACH REFLECTION

REFLECTIVITY OF VDA = 90%

——— CORRECT VALUE OF RE. INCLUDES CUMMULATIVE LOSS FROM MULTIPLE REFLECTIONS.

- - - - FICTITIOUS RE. VALUES THAT WOULD OCCUR IF ALL REFLECTED LIGHT WERE REFLECTED ONLY ONCE. (INCLUDED TO SHOW MAGNITUDE OF MULTIPLE REFLECTION LOSS EFFECT)

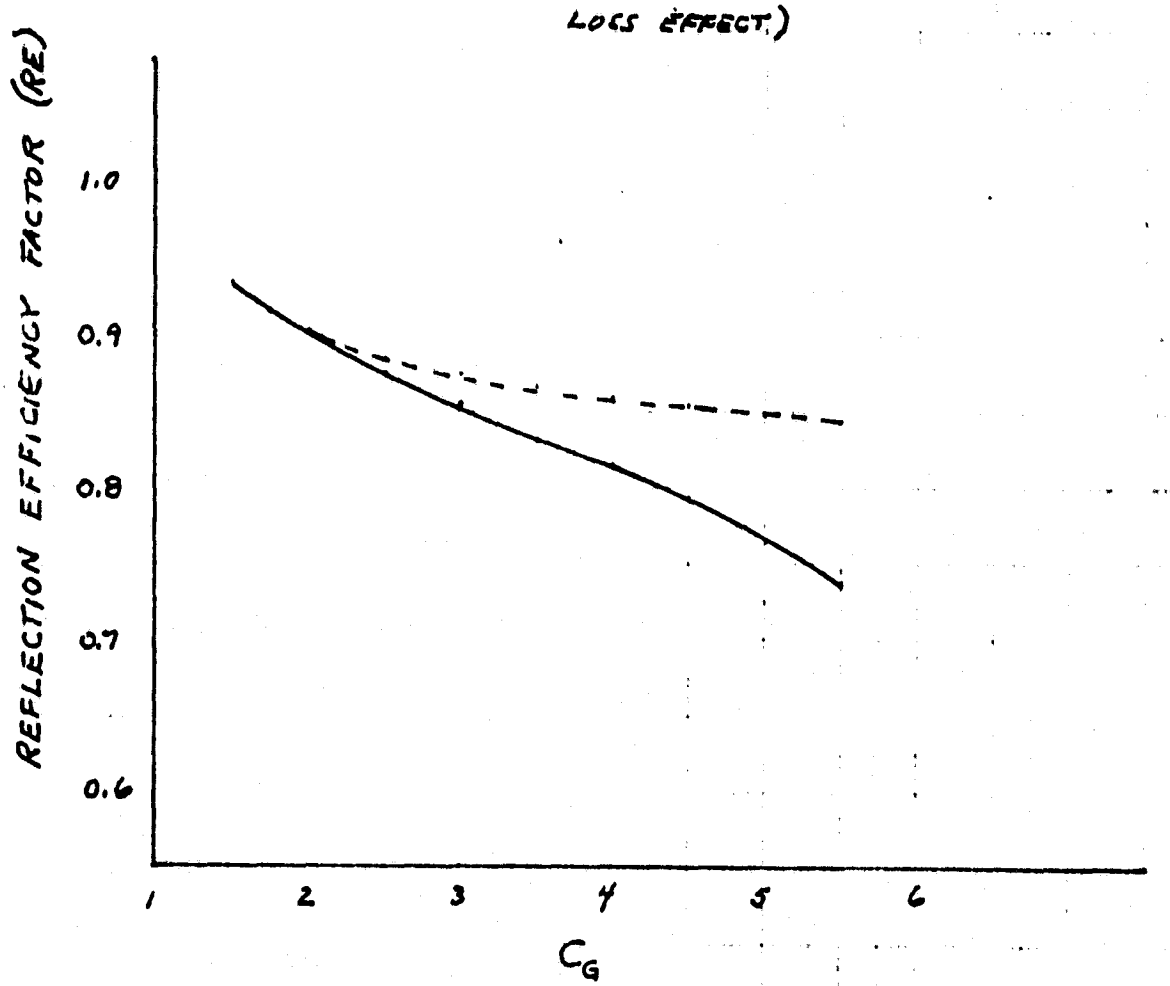

4.0 Thermal Analysis

The thermal analysis task during the contract extension period included the following:

- o Extension of the MFPC analysis, reported in the interim final report, to an array design utilizing GaAs solar cells at 1 AU.
- o Prediction of array temperatures for a GaAs flexible array at 1AU augmented by a 2D-FPT concentrator (Flat Plate Trough design) assuming either a VDA or "cold mirror" concentrator reflector finish, and
- o Prediction of array temperatures for a conventional (8 mil) silicon cell, rigid substrate array at 1AU augmented by the 2D-FPT.

The GaAs array temperature predictions for the MFPC design are given in Figure 4.1. The computational methods described in Ref. 1 were used to predict array temperatures for VDA and cold mirror reflector finishes. The latter case is shown parametrically with the effective coating reflectance in the wavelengths from which electrical power is generated. Spectral analysis of recent OCLI data indicates this reflectance is approximately 0.72 (See 5.0 Section). Solar cell open circuit solar absorptance (α_{oc} = .76) was taken as the average derived from the GaAs spectral reflectance measurements given in Figure 4.2. Cell efficiency, accounted for in the array thermal heat balance, was taken from data presented in Section 5.0. Total reflectance, transmittance, and emittance of the cold mirror and effective cell absorptance (reflected illumination) were derived from earlier OCLI data presented in Reference 1.

GaAs array temperature predictions at 1AU for a VDA 2D-FPT concentrator reflector are given in Figure 4.3 as a function of reflector tilt angle, $\emptyset$. The

concentrator configuration was assumed oversized to accommodate a $\pm$5 degree sun alignment error with multiple reflections. Concentration ratios and multiple reflection patterns, accounted for in the analysis, are given as a function of $\emptyset$ in Section 3.0. Effects of cell output degradation after 10 years in geosynchronous orbit are also shown. This is based on efficiency degradation given in Section 5.0. Reflector loss caused by surface distortions was assumed to be 10 percent. This loss was applied to each successive reflection in those cases where multiple reflections occur. Array backside emittance was assumed to be 0.8. Temperature difference across the array thickness was neglected. Similar results are given in Figure 4.4 for a cold mirror reflector finish. These predictions were based on cold mirror total reflectance, transmittance, and effective cell absorptance values derived from the OCLI coating spectral data given in Figs. 4.5 & 4.6. The coating emittance was assumed to be 0.5, that of the substrate. Effects of infrared thermal backloads from the reflectors to the array are relatively small ($\leq 10^{o}$C) for either reflector finish and were estimated by the technique described in Reference 1.

Array temperature predictions for a conventional silicon cell, rigid array at 1AU with a 2D-FPT concentrator are shown in Figure 4.7 for VDA and cold mirror reflector finishes.

Cell properties ($\sim$ K6 3/4) defined in Reference 1 were assumed. The aluminum honeycomb array substrate, described in Section 7, was assumed to be approximately 5/8 in. thick, 3/6 in. cell aluminum honeycomb core with aluminum facesheets, having a through thickness thermal conductance of 13 Btu/hr-ft^2 ^{o}F. The array backside emittance was taken as 0.8.

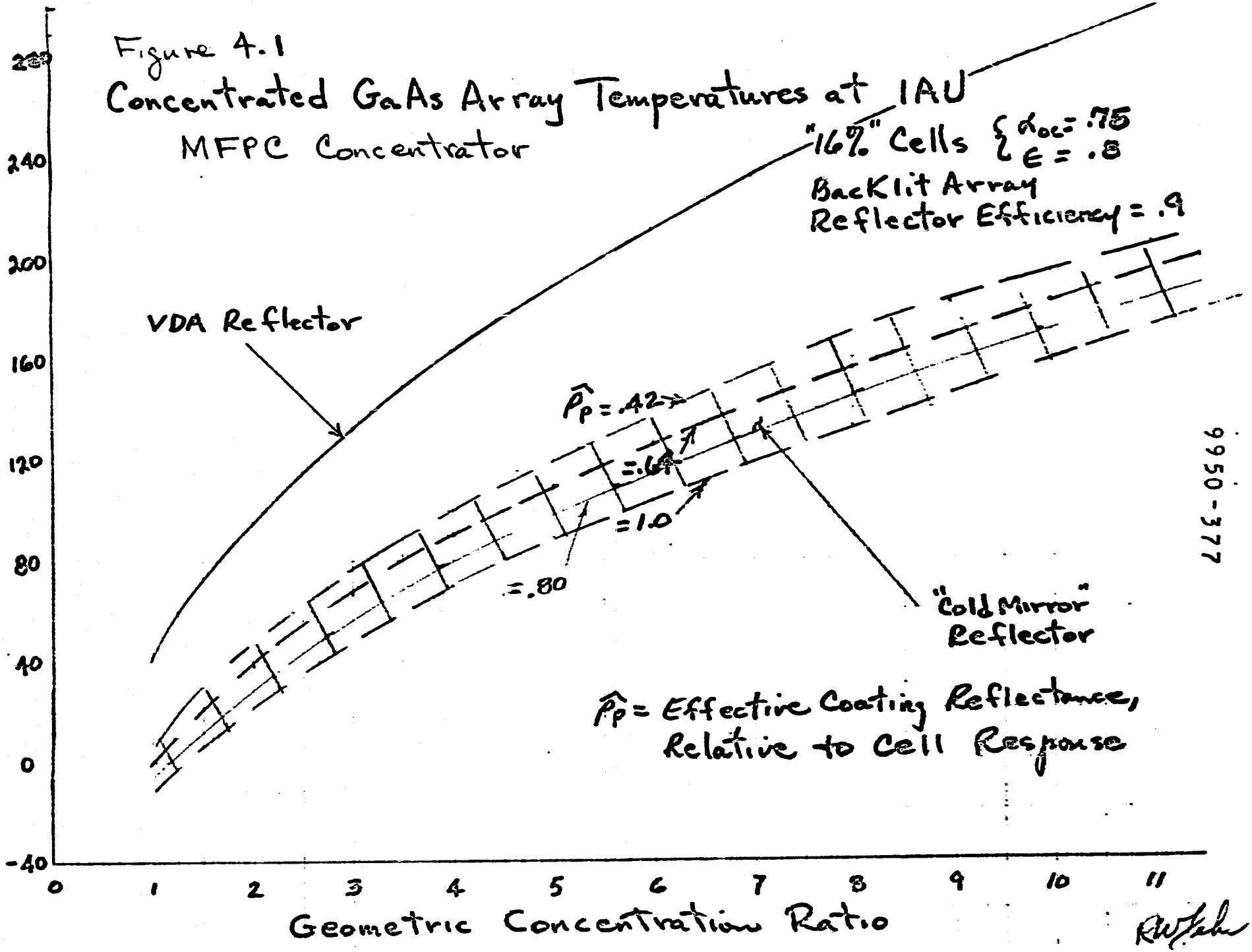

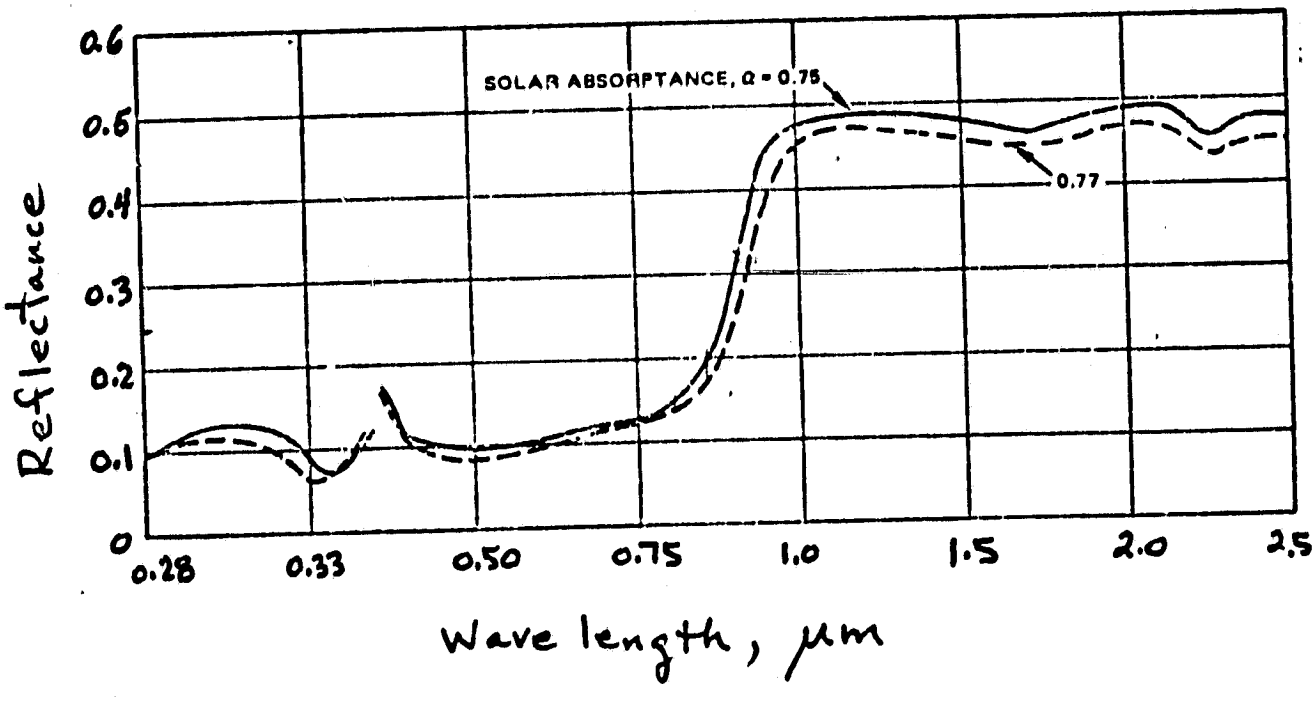

Figure 4.2 GaAs Solar Cell Spectral Reflectance (12 mil 7940 Cover Glass)

54

Figure 4.3 9950-377

GaAs Solar Array Temperatures with 2D-FPC Concentrator

VDA Reflector Finish ($\rho = .9$)

Concentrator Distortion Loss = .1

Concentrator Oversized for ±5° Sun Misalignment (OPTION ①)

Geosynchronous Orbit

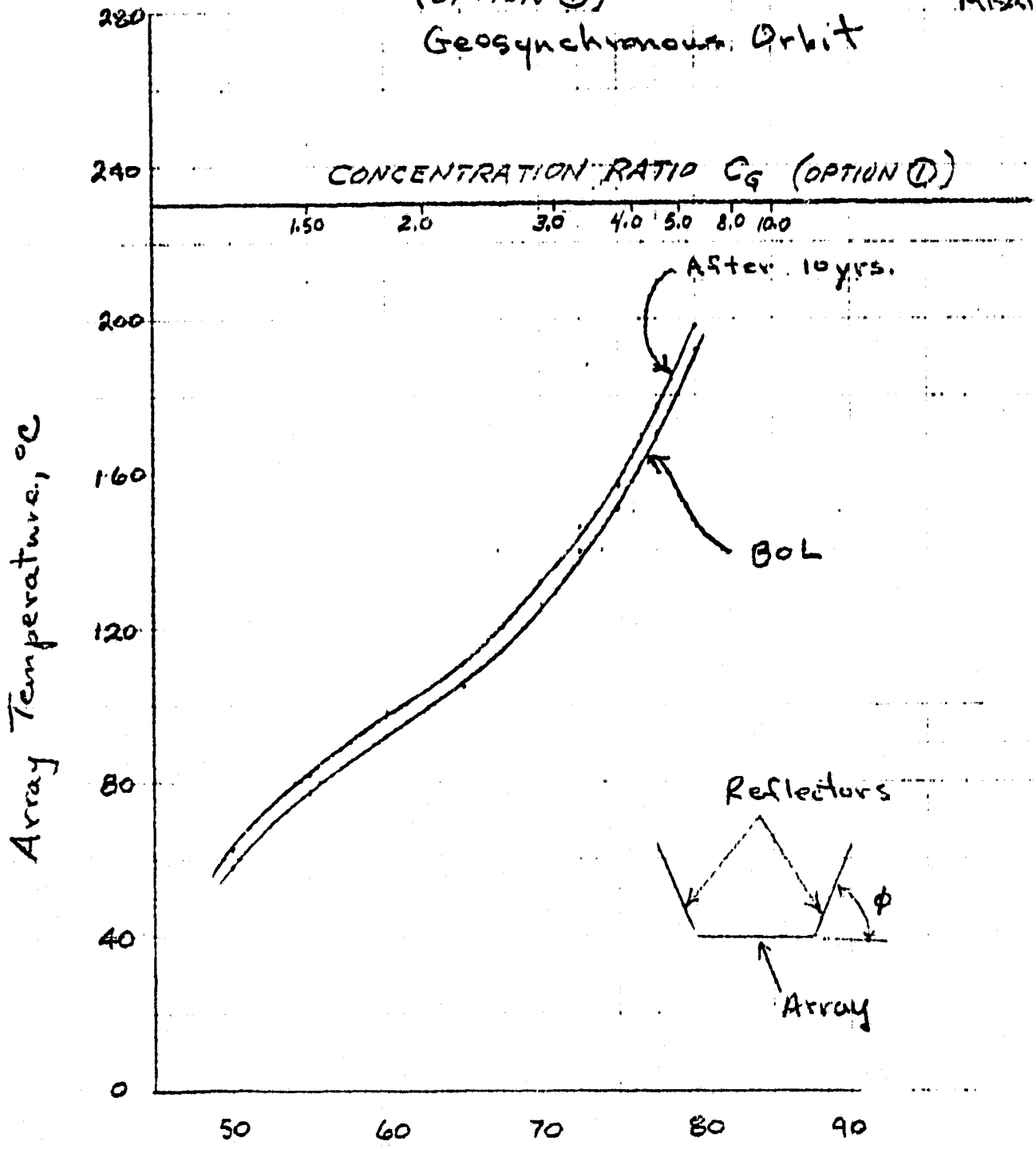

10/1/79

Figure 4.4 9950-377

GaAs Solar Array Temperatures with 2D-FPL Concentrator

"Cold Mirror" Reflector Finish ($\rho \sim .48$)

Concentrator Distortion Loss = .1

OPTION ① → Concentrator Oversized for ±5° Sun Misalignment

Geosynchronous Orbit

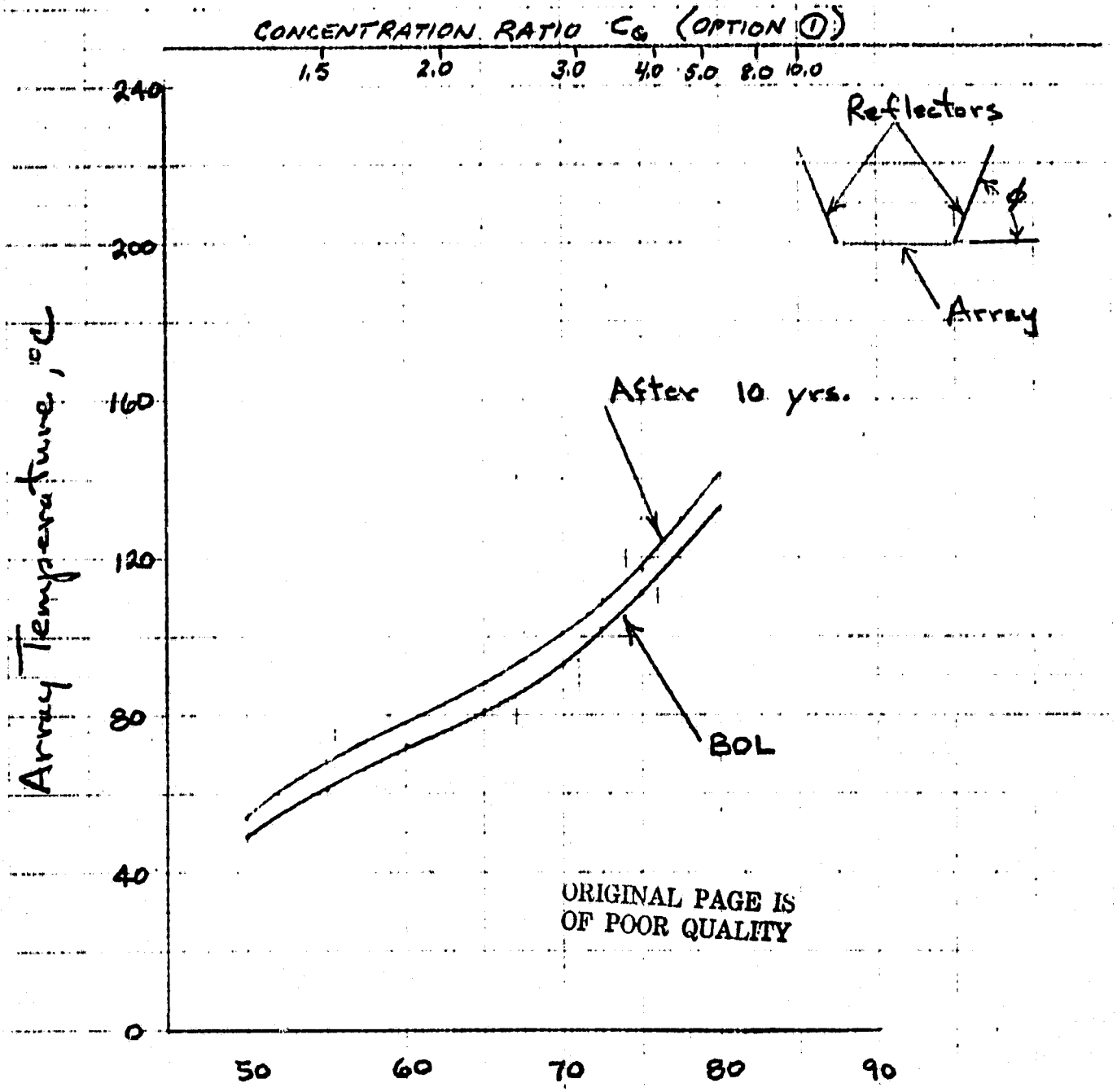

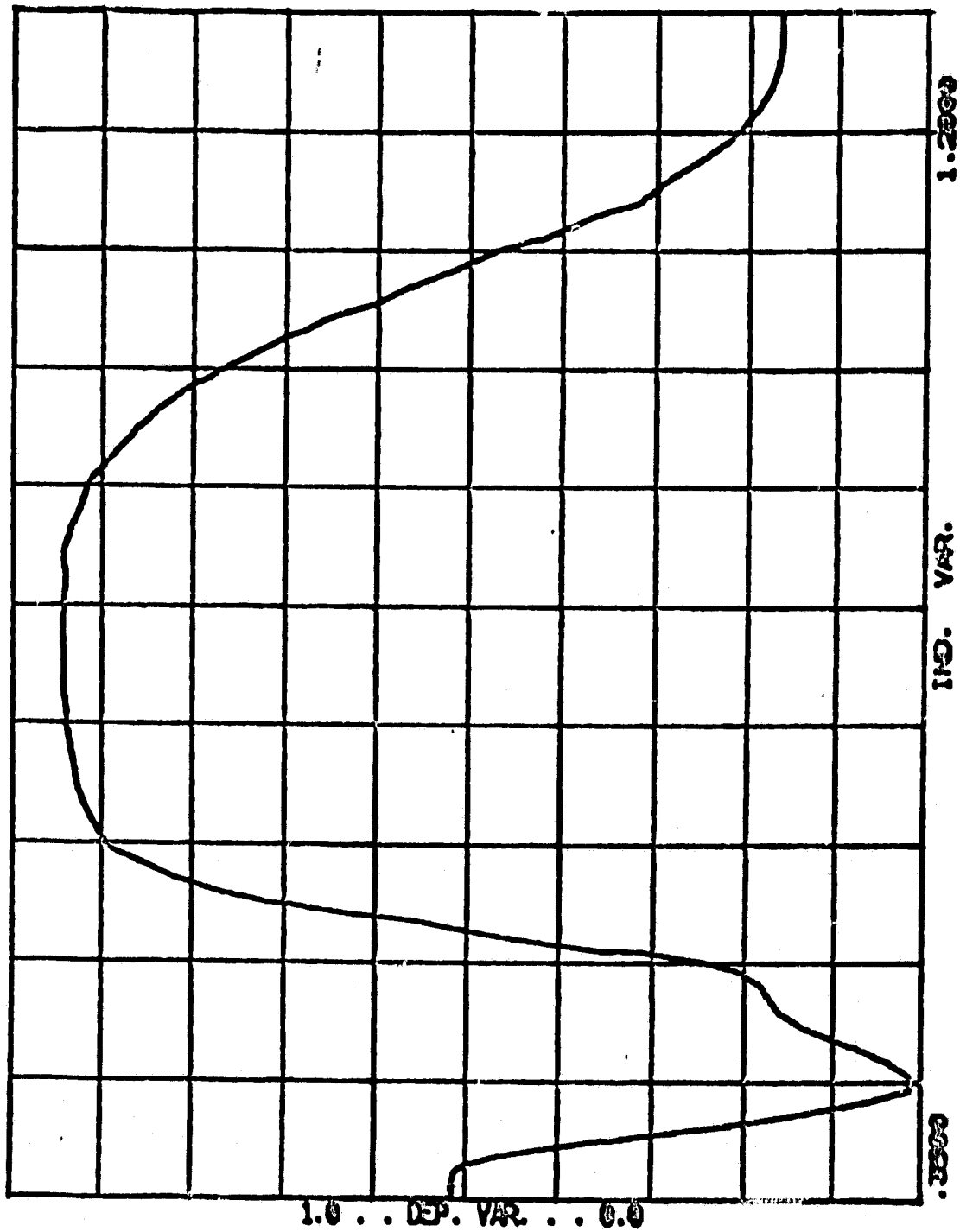

Figure 4.5 OCLI Cold Mirror Spectral Reflectance

Reflectance

Wavelength, μm

Figure 4.6 OCLI Cold Mirror Spectral Transmittance

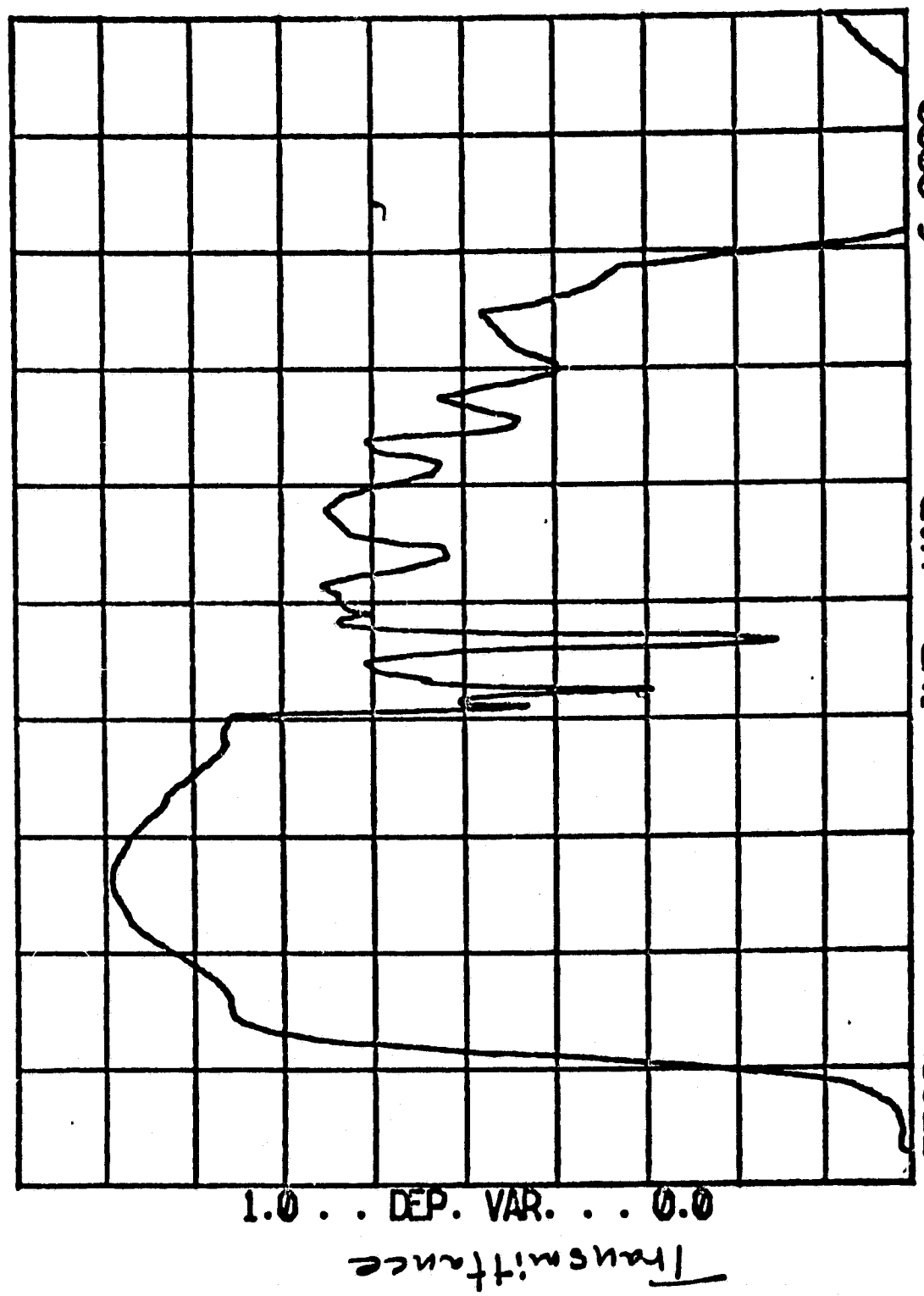

Figure 4.7
Rigid Si Solar Array Temperatures with 2D-FPC Concentrator

Concentrator Distortion Loss = .1

OPTION ① → Concentrator Oversized for ±5° Sun Misalignment
Geosynchronous Orbit

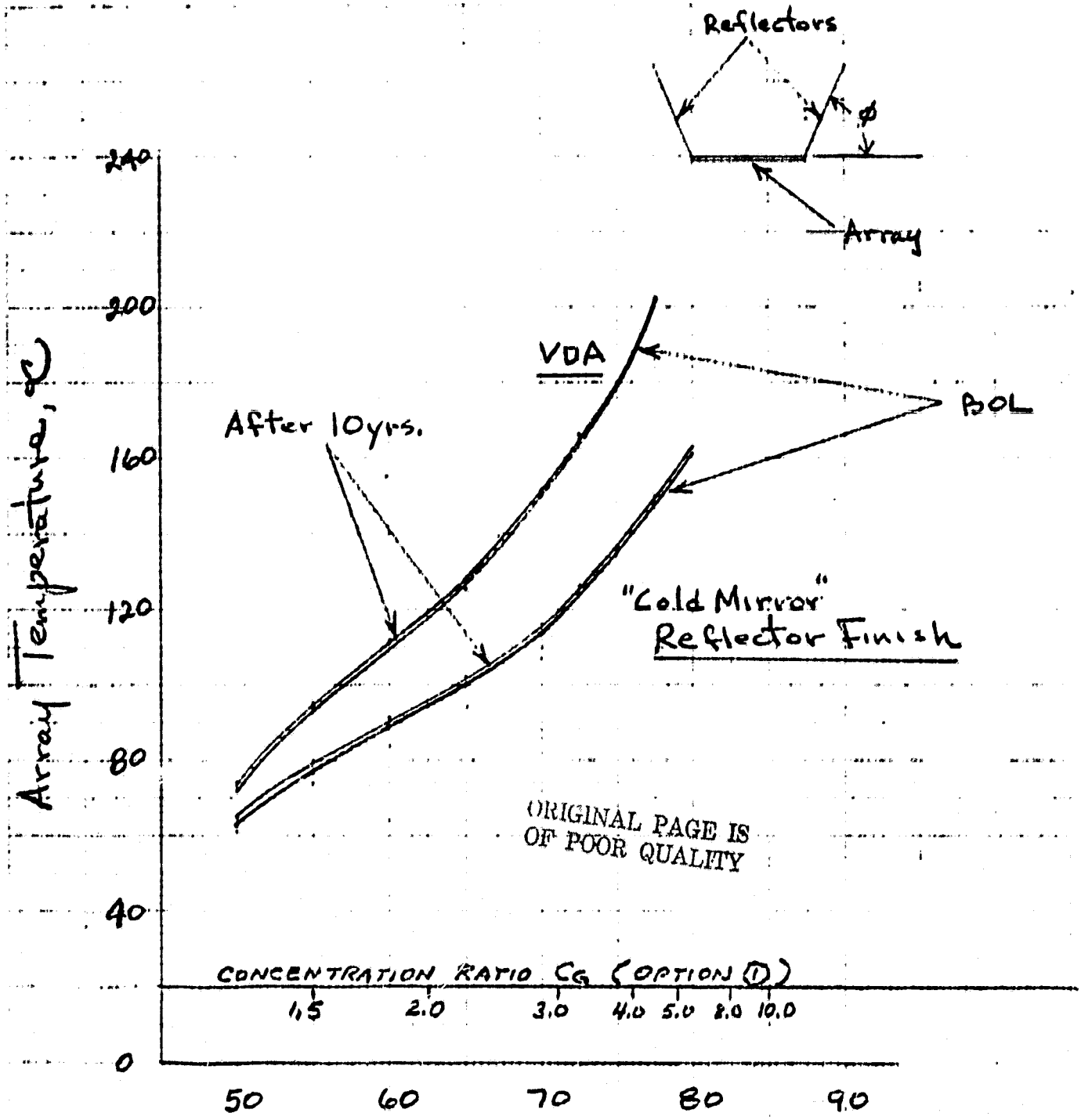

R. W. Fahrenheit 10/4/79

5.0 Solar Cell Analysis

The scope of this task during the first extension phase of the subject contract was limited to the performance of one specific silicon and one specific gallium arsenide solar cell for which Hughes has actual test data.

5.1 Baseline Cell Description

5.1.1 Silicon Solar Cell

Base resistivity	10 Ω cm
Junction depth	Shallow
Back surface field	No
Back surface reflector	Yes
Sculpture	No
Anti-reflection coating	Dual AR
Efficiency @ 28°C	13%
Life	10 Years
Cell thickness	0.008 in.
Cover material	Fused silica
Cover thickness	0.006 in.
Temperature	55°C
Orbit	Synchronous

5.1.2 Gallium Arsenide Solar Cell

Window	0.5 μm *
Growth	Liquid Epitaxial
Anti reflection coating	Ta_2O_5
Thickness	0.002 in.
Cover	
Material	Fused silica
Thickness	0.003

* GaAs cells are currently being made with thinner windows, between 0.1 and 0.2 μm.

5.1.2 Cont'd

Efficiency @ 28°C	16%
Temperature	55°C
Life	10 years
Orbit	Synchronous

5.2 Radiation Effects

The synchronous radiation environment was taken from the JPL Radiation Handbook 77-56. No solar proton effect was taken into account since that phenomena is launch date dependent. Taking into account the front and back side shielding, the following represent the assumed annual equivalent 1 MEV fluence at the cell junction.

	Si	Ga
front	3.14E13	4.77E13
back	2.5E13	4.77E13
Total	5.64E13	9.54E13

The silicon solar cell degradation was then taken directly from figure 3-58 of the referenced handbook. The Gallium cell degradation data was taken from limited radiation testing performed by JPL for HAC. Theory would say that the Ga cell should have superior radiation performance than Si. However, the limited testing to date on a 0.5 μm window cell has shown a performance very similar to that of a 10 cm back surface field cell. This performance is inferior to that of a conventional 10 Ω-cm cell and would improve as the window layers were decreased to between 0.1 and 0.2 μm.

5.3 Temperature Effects

The temperature coefficients for Si were derived from fig. 3.16 of the referenced handbook taking into account the radiation dependence. Only limited Ga data on unirradiated cells is available at this time so the temp coefficient ($\sim$ ½ that of Si) was held constant during the 10 year life. (As shown in Fig 3-16, JPL Rad. Handbook) the temperature dependence decreases with increased radiation dosage thus accounting for the BOL & EOL curves crossing over.

5.4 Results

The efficiencies, corrected for temperature and as a function of radiation dose, are shown below for the 55° case. These data, including temperature coefficient data are plotted in Figs. 5.0-1, 5.0-2 and 5.0-3. Although the Ga degrades more rapidly than the Silicon cell its end of life performance at 55°C is still substantially better than the Si performanc .

1 MeV Electrons	Efficiency at 55°C	
	Si	Ga
0	11.1	14.8
10^{13}	11.1	14.6
10^{14}	11.04	13.7
10^{15}	9.76	11.1

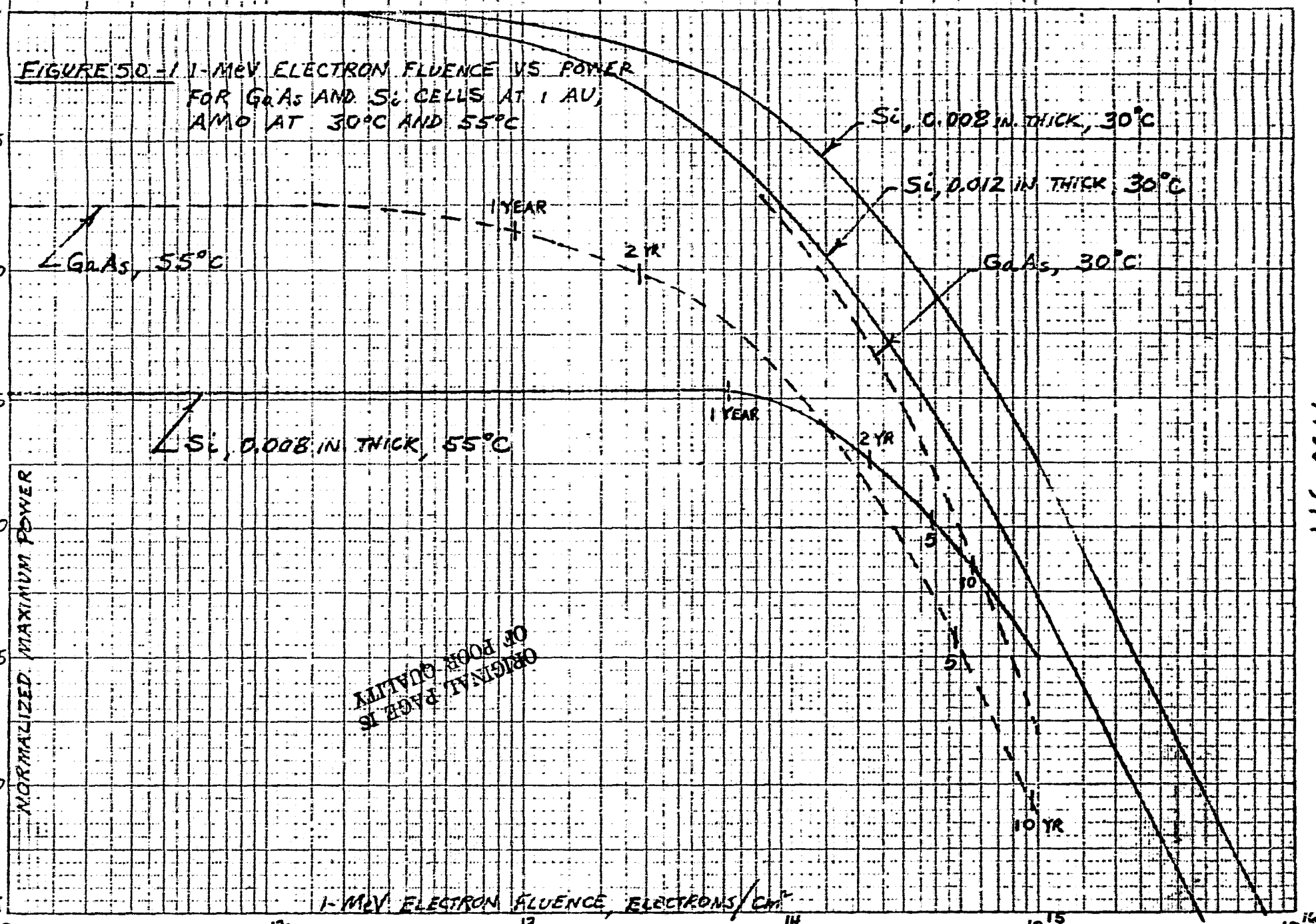

YEARS @ 55°C

FIG. 50-2

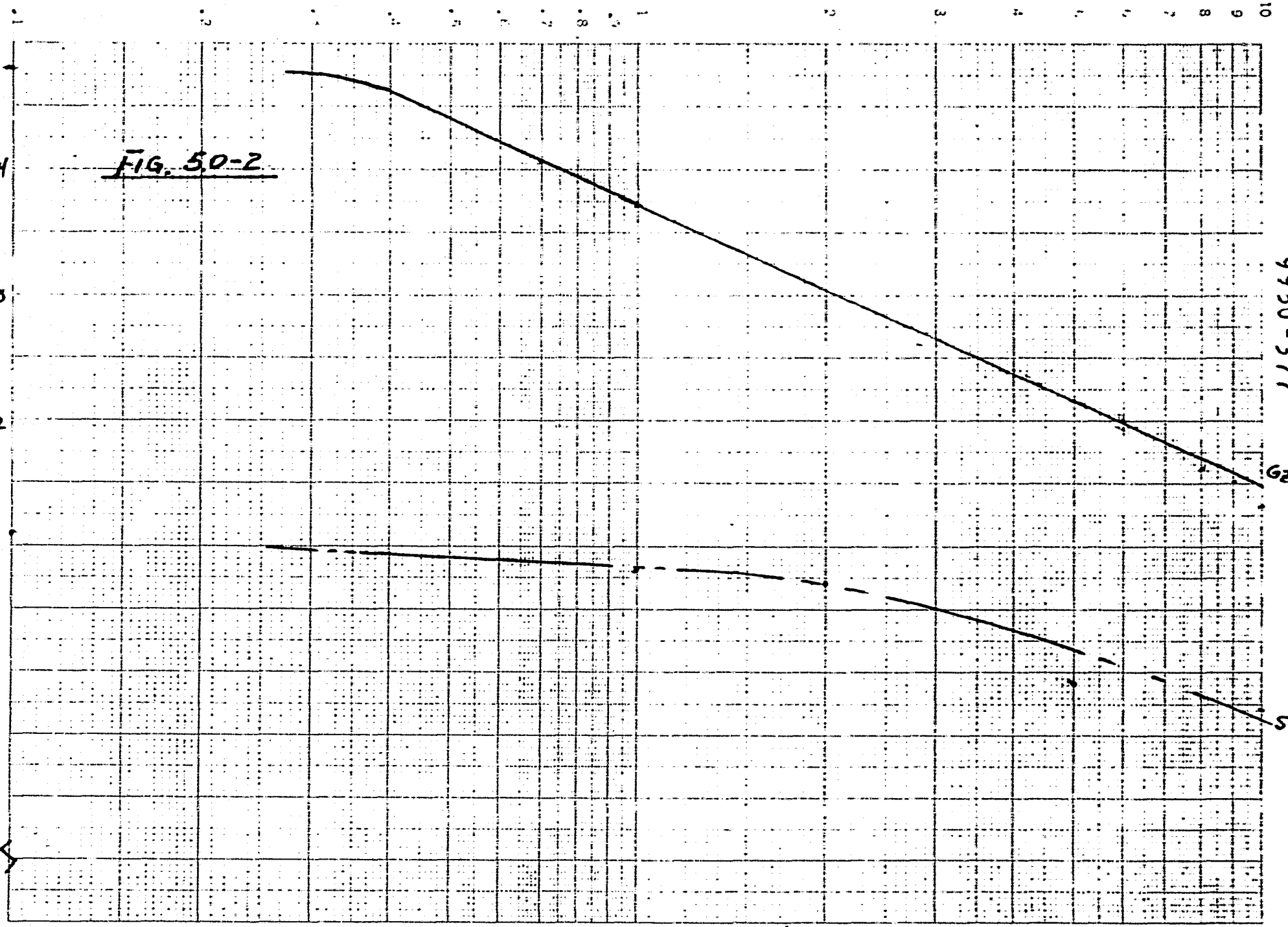

9950-377

SOLAR CELL EFFICIENCY COMPARISON

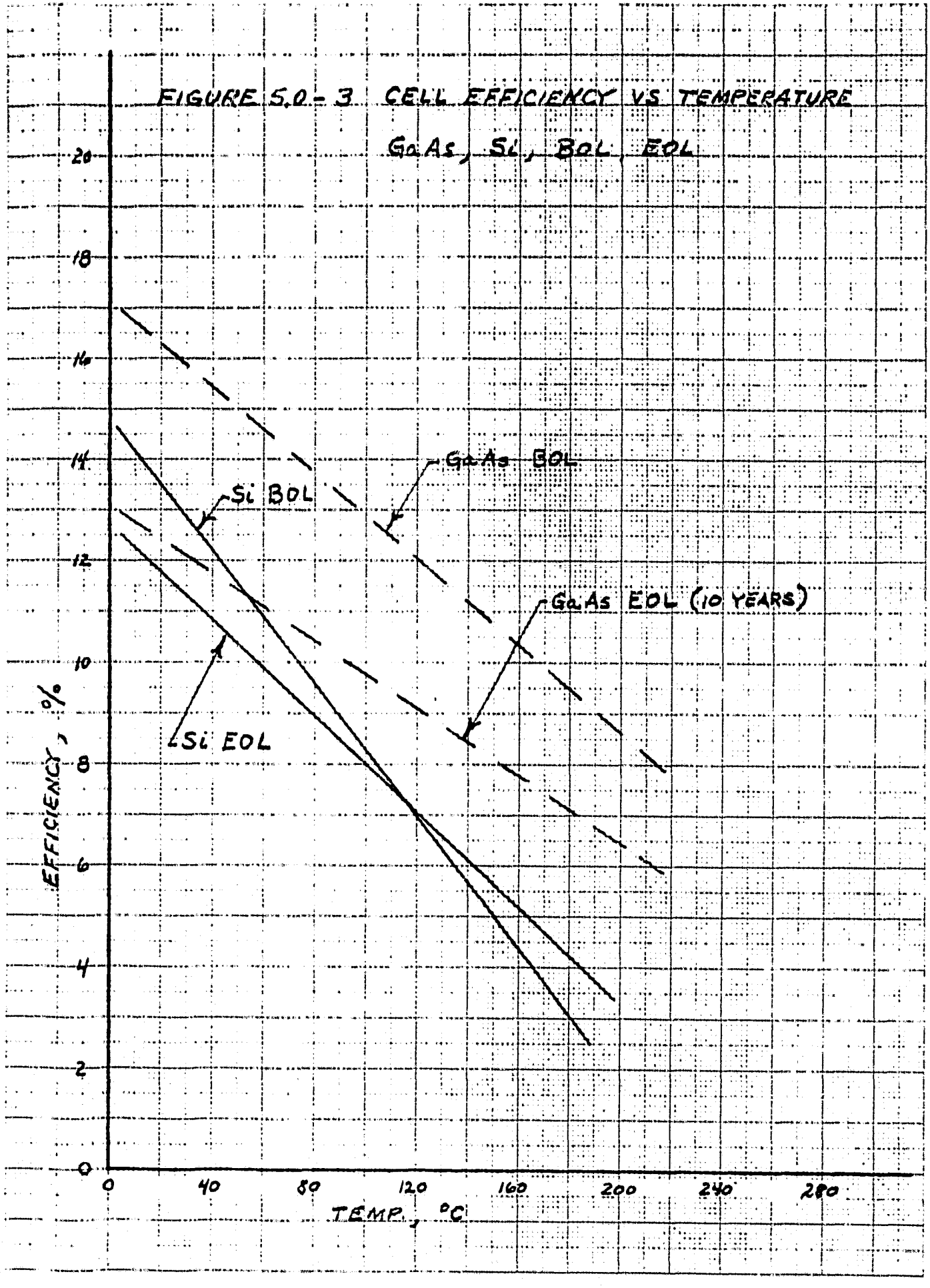
FIGURE 5.0-3 CELL EFFICIENCY VS TEMPERATURE
GaAs, Si, BOL, EOL
GaAs BOL
Si BOL
GaAs EOL (10 YEARS)
Si EOL
EFFICIENCY, %
TEMP, °C
0
2
4
6
8
10
12
14
16
18
20
0
40
80
120
160
200
240
280

6.0 System Evaluation

For each design configuration that was considered, the primary system evaluation task was to determine the required area of the array and of the concentrator mirrors for each value of C_g such that the system would generate 2KW of power after 10 years in geosynchronous orbit. All computations were initially carried out on a per unit area basis.

As a starting point it was necessary to find the unconcentrated BOL and EOL power per square foot for each of the two solar cell arrays specified by the contract statement of work. First for a conventional, thick Silicon array on a rigid honeycomb substrate and then for a thin GaAs array on a thin flexible substrate. These initial unit power calculations were based on 55°C temperature, AMO, geosynchronous orbit. The basic formulae employed to find P, the power per unit area before concentration, is

P = Solar constant x Cell operating efficiency x Packing factor x loss factors.

A 90% packing factor was used and the loss factors employed were .97 for assembly loss, .96 bussing loss and .995 diode loss.

Thus, using the cell efficiency data presented in Section 5.0, for the silicon array,

$$P_{BOL} = 135.3 \times 0.111 \times .90 \times .97 \times .96 \times .995$$

$$= 12.52 \frac{mw}{cm^2}$$

$$= \underline{\underline{11.61 \frac{watts}{ft^2}}} \text{ BOL}$$

$$P_{EOL} = \frac{.0966}{.111} \times 11.61 = \underline{\underline{10.1 \text{ watts/ft}^2}} \text{ EOL}$$

and for the GaAs array,

$$P_{EOL} = 135.3 \times .148 \times .90 \times .97 \times .96 \times .995$$

$$= 16.7 \frac{mw}{cm^2} = \underline{\underline{15.51 \text{ watts/ft}^2}} \text{ BOL}$$

$$P_{EOL} = 15.51 \times \frac{.113}{.148} = \underline{\underline{11.84 \frac{watts}{ft^2}}} \text{ EOL}$$

To size the array for the concentrated system parametrically, the following expression was used:

$$2000 \text{ watts} = A \times P_{EOL} \times C_g \times (RE) \times \frac{N_{temp}}{N_{55^oEOL}}$$

where:

A = area of the array required, ft^2 (The dependent variable)

P_{EOL} = End of life power per unit area at 55°C, $watts/ft^2$

C_G = Geometric concentration ratio (the independent variable)

(RE) = Reflection efficiency from figure 3.0-11 or 3.0-12, a function of C_g and mirror coating considered.

N_{temp} = End of life cell efficiency from section 5.0 evaluated at the predicted end of life cell temperature from section 4.0, a function of C_g and mirror coating.

N_{55^oCEOL} = End of life cell efficiency at 55°C, from section 5.0

The results of this procedure, as described, are shown in figure 6.0-1 for 2D-FPT (V trough) designs and in figure 6.0-2 for the MFPC designs. In all cases, optimum concentration to produce maximum array area reduction is indicated by the "knee" of these curves. At concentrations in excess of these values, temperature effects on the efficiency of the cells produce diminishing returns.

Clearly, the most dramatic reductions in required array areas produced by concentration, occur in the Gallium Arsenide concepts. With VDA coated mirrors the maximum reduction in array area is almost identical in the 2D-FPT and MFPC designs; 55% and 58%, both occurring at the same concentration ratio of about 5.5. With the improved cold mirror coating, a 77% reduction

results with the MFPC but no improvement over the VDA is found in the 2D-FPT because of the effect of multiple reflections inherent in this concept. (See Section 3.0).

In the Silicon solid substrate array concept, the maximum reduction in array area is minimal with the VDA coated mirrors; only 13% at $C_g = 2.5$. The cold mirror coating here produces a somewhat improved result with 27% reduction at $C_g = 3.0$. The greater sensitivity of the silicon cell to temperature effects account for its poorer showing as compared to Gallium Arsenide.

FIGURE 6.0-1 ARRAY AREA VERSUS CONCENTRATION RATIO
2D-FPT DESIGN CONCEPTS
1 AU, 2KW OUTPUT EOL

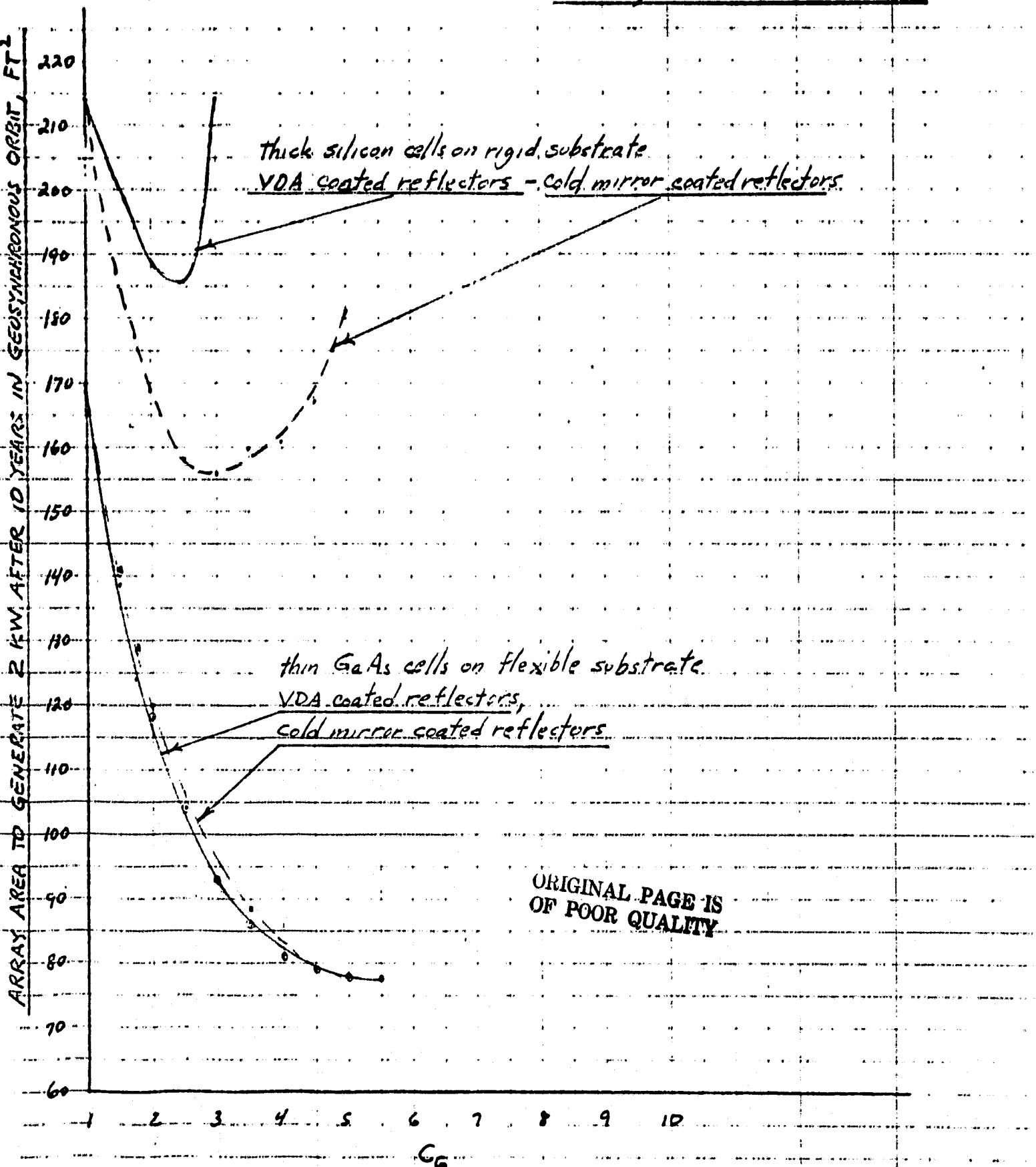

FIG. 6.0-2 REQUIRED ARRAY SIZE FOR 2 KW OUTPUT MEPC IN GEOSYNCHRONOUS ORBIT WITH THIN GaAs CELLS

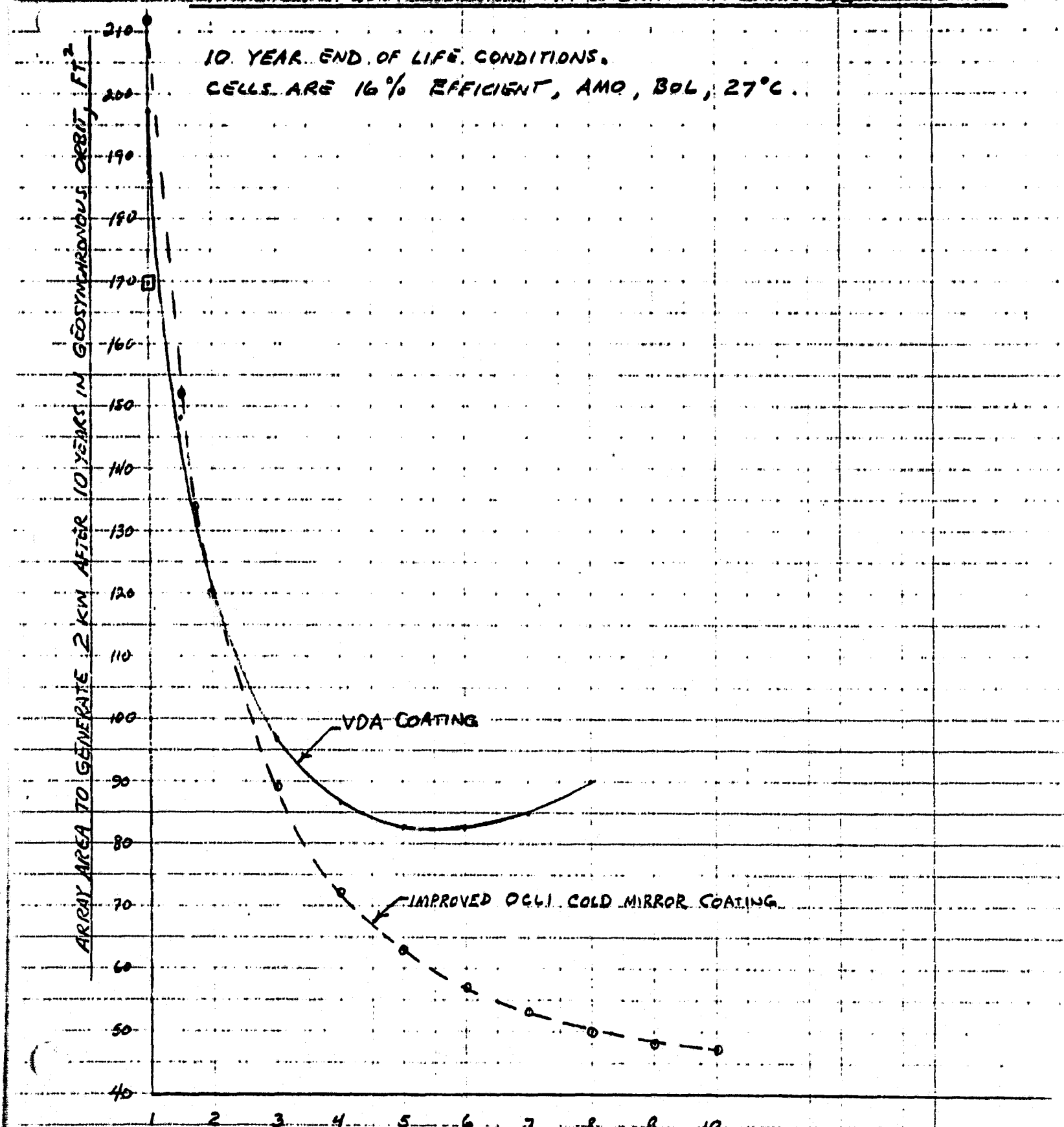

7.0 Weight Estimates

To determine specific power of the various concepts studied, it was necessary to estimate the total system weight of each concept as a function of the geometric concentration ratio.

MFPC Concepts

For the semi-active version, this was accomplished by using as a baseline or starting point, the detailed weight breakdown for the specific MFPC design presented in Vol. 2 of the interim final report. Here, the total weight of the system is 196 lbs. when:

the array area = 173 sq. ft.

$C_g = 16$

array density = $\frac{22.8 \text{ lbs.}}{173 \text{ ft}^2} = 0.132 \text{ lb/ft}^2$, (thin silicon cell).

On the other hand, for each point on the required weight vs. C_g curve for the geosynchronous 2 kW MFPC version, a different array area was required at a slightly different density (0.189 lb/ft^2, thin GaAs cell). Also, each point required a different and lower C_g than the 16 used in the baseline weight breakdown and thus a smaller number of mirrors. By grouping the items in the baseline weight breakdown by those that would be proportional to array area and density; those that would be proportional to the number and size of mirrors; and those that would tend to be almost constant with changes in these parameters, it was possible to estimate the final system weight for each point on the required curve.

Weight for the passive version of the 2 kW geosynchronous MFPC were obtained by a ratio process in which the weight versus C_g curves for these versions as obtained during phase I of the contract were employed. The ratio of the weights of the passive and active versions at each C_g as obtained from these curves was used as a multiplying

factor to convert the active MFPC geosynchronous weight data to the corresponding passive weights.

2D-FPT (V-Trough) Concepts

Two V-trough design concepts were considered in the first extension phase of the contract. One was a fully deployable system employing thin Gallium Arsenide cells on a light weight flexible substrate in which both reflector mirrors and the array are wound on a drum. The other design concept simply involved the addition of mirrors and mirror support and deployment hardware to an existing rigid (non-furlable) silicon solar array. Both designs were conceptualized sufficiently to permit rough or first cut weight estimates to be generated as a function of concentration ratio (hence as a function of mirror and array size). In both designs, the array area was adjusted for each concentration ratio investigated such that a constant power output of 2 kW at 10 years end of life is generated. Figure 7.0-1 is a simple illustration of one wing (half of a 2 wing 2 kW pair) of the flexible drum wound Gallium Arsenide array after deployment.

Prior to stowage, the reflector film is accordian folded over the fully extended array. The reflector and array are then wound on a 20 inch nominal diameter drum. The drum length is equal to the full solar cell array width.

The drum wound array is then housed in a split cylinder. A telescoping rectangular graphite epoxy deployment mast is fixed to the drum array support cylinder half. The deployment procedure begins with the extension of this mast. This mast is not a conventional astro mast type but is rather an original Hughes design concept which Hughes believes to be considerably more weight efficient and rigid than an astro mast. Extension of this mast is also an original Hughes design concept in which a two sheave cable belt reciprocating drive is utilized. Segments are rigidly locked as deployed with the final segment sprung rather than locked to maintain required tension. In a

similar manner, the reflector is deployed by sequential extension of masts and cross arms fixed to each of the housing cylinder halves. For maximum stiffness to mass ratios, graphite epoxy resin construction is assumed for all structural members.

The rigid substrate silicon array concept began with a substrate defined by the contract extension statement of work. This consisted of a sandwich construction with aluminum face plates and honeycomb core, similar to the FLTSATCOM array. The specified rigid array, unconcentrated, was found to weigh 0.88 lbs. per square foot of area.

In both 2D-FPT concepts, the mirror lengths for each concentration ratio were based on the optimum lost light design configuration described in Section 3.0, while the array areas required were obtained as described in Section 6.0. The effect of the improved cold mirror reflector coating as compared to the ordinary aluminum mirror (VDA) was included in the weight estimates. The results of the weight calculations are summarized in Figure 7.0-2.

In this figure, all of the weight versus concentration ratio curves for the concepts studied exhibit, initially, a decreasing total weight with increasing concentration. As the concentration goes up; the array area hence array length and weight required to produce 2 kW EOL goes down. Of course, the mirror width increases to produce higher concentration but this is offset, initially, by the decreasing trough length. However, as concentration is further increased, the required mirror width and thus support structure weight begins increasing more rapidly because of the optics, while the array area begins decreasing less rapidly due to thermal effects. In every case, the result is a knee in the weight curve at relatively low concentration (between C_g = 2.5 to 3.0).

FIGURE 7.0-1 FLEXIBLE SUBSTRATE ARRAY

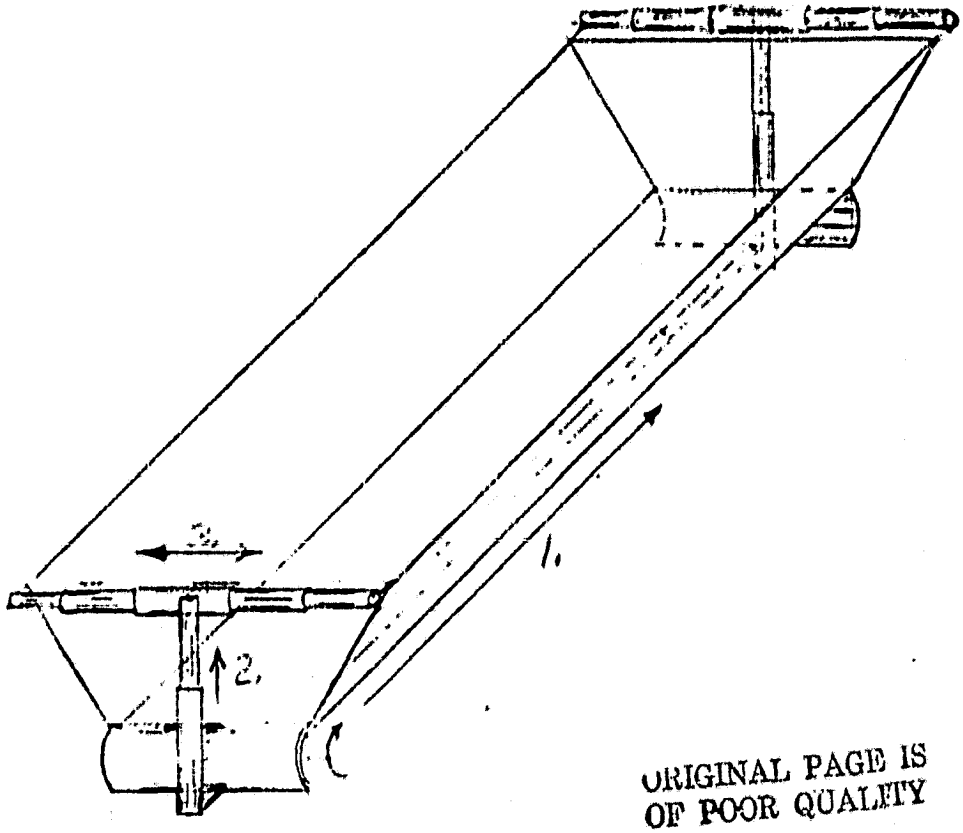

NOTE: ① TELESCOPING MEMBERS ARE GR/E 1.0" NOMINAL DIAMETER GOLD PLATED BERYLLIUM COPPER ELLIPTICAL PNEUMATIC TUBE FOR RECTANGULAR BOOM

② FOR RIGID SUBSTRATE REFLECTOR IS FOLDED ACCORDION STYLE OVER PANEL FOR STOWAGE

FIGURE 7.0-2. ESTIMATED WEIGHT VS C_G OF CONCEPTS STUDIED
ALL WITH 2KW CONCENTRATED POWER, EOL, 1 AU